

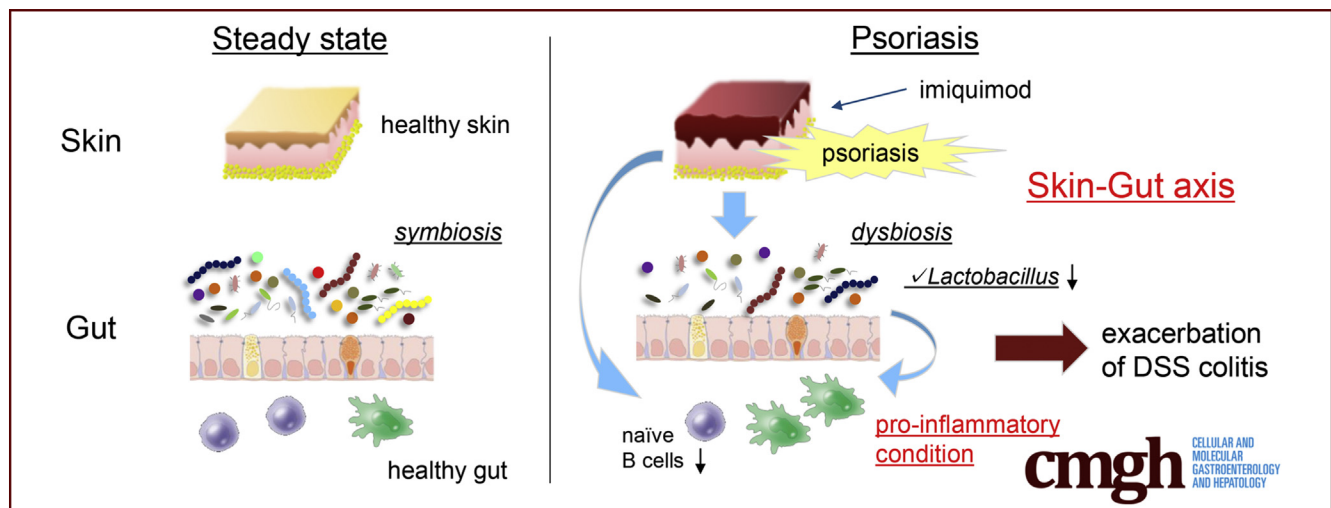
## ORIGINAL RESEARCH

## Toll-Like Receptor 7 Agonist–Induced Dermatitis Causes Severe Dextran Sulfate Sodium Colitis by Altering the Gut Microbiome and Immune Cells



Hiroki Kiyohara,<sup>1</sup> Tomohisa Sujino,<sup>1,2</sup> Toshiaki Teratani,<sup>1</sup> Kentaro Miyamoto,<sup>1,3</sup> Mari Mochizuki Arai,<sup>1</sup> Ena Nomura,<sup>1</sup> Yosuke Harada,<sup>1</sup> Ryo Aoki,<sup>1,4</sup> Yuzo Koda,<sup>1,5</sup> Yohei Mikami,<sup>1</sup> Shinta Mizuno,<sup>1</sup> Makoto Naganuma,<sup>1</sup> Tadakazu Hisamatsu,<sup>1</sup> and Takanori Kanai<sup>1,2</sup>

<sup>1</sup>Division of Gastroenterology and Hepatology, Department of Internal Medicine, Keio University School of Medicine, Tokyo, Japan; <sup>2</sup>Japan Agency for Medical Research and Development, AMED, Tokyo, Japan; <sup>3</sup>Miyarisan Pharmaceutical Co, Ltd, Tokyo, Japan; <sup>4</sup>Institute of Health Sciences, Ezaki Glico Co, Ltd, Nishiyodogawa, Osaka, Japan; <sup>5</sup>Tanabe Mitsubishi Pharmaceutical Co, Ltd, Tokyo, Japan



## SUMMARY

Dermatitis induced by Toll-like receptor 7 agonist accelerates dextran sulfate sodium colitis accompanied with decreased naïve B cells and a perturbed microbiome with reduced *Lactobacillus* species in the gut. We show the skin-gut axis is associated with the gut microbiome.

**BACKGROUND & AIMS:** Psoriasis and inflammatory bowel disease (IBD) are both chronic inflammatory diseases occurring in the skin and gut, respectively. It is well established that psoriasis and IBD have high concordance rates, and similar changes in immune cells and microbiome composition have been reported in both conditions. To study this connection, we used a combination murine model of psoriatic dermatitis and colitis in which mice were treated topically with the Toll-like receptor 7 agonist imiquimod (IMQ) and fed dextran sulfate sodium (DSS).

**METHODS:** We applied IMQ topically to B6 mice (IMQ mice) and subsequently fed them 2% DSS in their drinking water. Disease activity and immune cell phenotypes were analyzed,

and the microbial composition of fecal samples was investigated using 16S ribosomal RNA sequencing. We transplanted feces from IMQ mice to germ-free IQ1/Jic (IQ1) mice and fed them DSS to assess the effect of the gut microbiome on disease.

**RESULTS:** We first confirmed that IMQ mice showed accelerated DSS colitis. IMQ mice had decreased numbers of IgD<sup>+</sup> and IgM<sup>+</sup> B cells and increased numbers of non-cytokine-producing macrophages in the gut. Moreover, the gut microbiomes of IMQ mice were perturbed, with significant reductions of *Lactobacillus johnsonii* and *Lactobacillus reuteri* populations. Germ-free mice transplanted with feces from IMQ mice, but not with feces from untreated mice, also developed exacerbated DSS colitis.

**CONCLUSIONS:** These results suggest that skin inflammation may contribute to pathogenic conditions in the gut via immunologic and microbiological changes. Our finding of a novel potential skin-gut interaction provides new insights into the coincidence of psoriasis and IBD. (*Cell Mol Gastroenterol Hepatol* 2019;7:135–156; <https://doi.org/10.1016/j.jcmgh.2018.09.010>)

**Keywords:** Inflammatory Bowel Disease; Dermatitis; Gut Microbiome.

More than 100 trillion intestinal bacteria inhabit the human digestive tract, and interactions between bacteria and the host immune system play significant roles in both homeostatic and disease processes. Perturbations in the gut microbiome can contribute both to intestinal disorders, such as inflammatory bowel disease (IBD), as well as systemic diseases, including obesity, type 2 diabetes, atherosclerosis, and multiple sclerosis. Gut microbes affect the host immune system and vice versa: for instance, some *Clostridium* species can induce regulatory T cell (Treg) differentiation, and segmented filamentous bacteria can induce T helper (Th)17 cell differentiation. Moreover, it has been shown that interleukin (IL)10 knockout mice are colonized by colitogenic microbes and develop spontaneous colitis.

Psoriasis is a chronic dermatitis with a prevalence of 2%–4% in Western countries and 0.9%–8.5% worldwide.<sup>1</sup> Psoriasis and IBD share similar immunologic features,<sup>2–4</sup> and polymorphisms in the *IL12b* and *IL23r* genes confer increased susceptibility to both conditions.<sup>5,6</sup> Therefore, a mechanistic relationship between these conditions has been suspected, and, indeed, these 2 diseases are known to overlap. The prevalence of IBD in psoriatic patients is 4 times higher than in the general population,<sup>7,8</sup> and the prevalence of psoriasis in patients with Crohn's disease is higher than in healthy subjects.<sup>9</sup> In addition to shared immunologic features, patients with IBD and psoriasis have similar gut microbial compositions.<sup>10,11</sup> Recently, it was reported that enteric viruses can activate plasmacytoid dendritic cells (pDCs) via Toll-like receptor (TLR)7 signaling to produce type I interferon (IFN), which then can ameliorate colitis.<sup>12</sup> Administration of TLR7 agonists induced IL22 production by group 3 innate lymphoid cells (ILC3s), and conferred increased resistance against colonization by vancomycin-resistant enterococcus.<sup>13</sup> Thus, TLR7 signaling in the intestine may be beneficial for gut homeostasis. These findings seemingly contradict the evidence that patient populations with psoriasis and IBD overlap. Topical application of a TLR7 agonist (imiquimod [IMQ]) induces dermatitis, a phenomenon that has been widely exploited as a murine psoriasis model.<sup>14–16</sup>

We applied IMQ topically and administered dextran sulfate sodium (DSS) enterally as murine models of psoriasis-like dermatitis and colitis murine models, respectively, and analyzed skin–gut interactions between immune cells and gut microbes. We showed that IMQ-induced psoriatic dermatitis accelerated the severity of DSS colitis. Moreover, IMQ dermatitis was associated with reduced numbers of IgD<sup>+</sup> and IgM<sup>+</sup> B cells in the gut and altered composition of the gut microbiome, with a marked reduction observed in *Lactobacillus* species. Fecal transfer from IMQ-treated mice, but not untreated mice, to germ-free (GF) mice resulted in exacerbation of DSS colitis after transfer. Identifying potential skin–gut interactions between the immune system and the gut microbiome in murine models may help us understand the coincidence of psoriasis and IBD and lead to improved treatments for patients with these conditions.

All authors had access to the study data and reviewed and approved the final manuscript.


## Results

### Murine Psoriasis-Like Dermatitis Induced Severe DSS Colitis

First, we investigated whether psoriasis-like dermatitis could induce spontaneous colitis in a murine model. We topically applied IMQ to the shaved backs of mice for 6 consecutive days, followed by 3 days of rest. This treatment was repeated for 2 cycles (IMQ mice). Vehicle alone was topically applied instead of IMQ to the control mice (Figure 1A). IMQ mice developed psoriasis-like dermatitis (Figure 1B and C) but the animals did not develop spontaneous colitis (Figure 1D). To investigate potential interactions between skin inflammation and colitis, we next subjected the IMQ mice to a chemical colitis model. IMQ mice were fed 2% (wt/vol) DSS in their drinking water for 7 days (IMQ-DSS mice) (Figure 1E). Compared with control (cont)-DSS mice, IMQ-DSS mice showed more severe clinical symptoms of colitis including body weight loss, shorter colon length, loose stool consistency, and gross bleeding. This phenotype was reflected in the increased disease activity indexes (DAIs) of these animals (Figure 1F–I). Histologic analyses of IMQ-DSS mice showed complete destruction of the epithelial layer, loss of crypts, submucosal edema, and intestinal inflammation with immune cell infiltrates; histologic scores were significantly higher in IMQ-DSS mice than in cont-DSS mice (Figure 1J and K). Taken together, these data showed that IMQ-DSS mice developed more severe colitis than cont-DSS mice.

To assess the immune cell composition of the colonic mucosa, we analyzed the frequencies of macrophages, B cells, and T cells in IMQ-DSS and cont-DSS mice by flow cytometry. Although macrophage frequency was comparable between the 2 groups, the proportion of CD80-expressing macrophages (M1-type macrophages) was slightly increased in IMQ-DSS mice (Figure 1L–O). The frequency of B cells in the colon was decreased significantly in IMQ-DSS mice, whereas the frequency of T cells in the colon was comparable between the 2 groups (Figure 1P–R). We found no differences in the frequencies of Th17 cells, Th1 cells, or Tregs between IMQ and control mice (data not shown). Interestingly, the numbers of IgD<sup>+</sup> and IgM<sup>+</sup> B cells were greatly decreased in

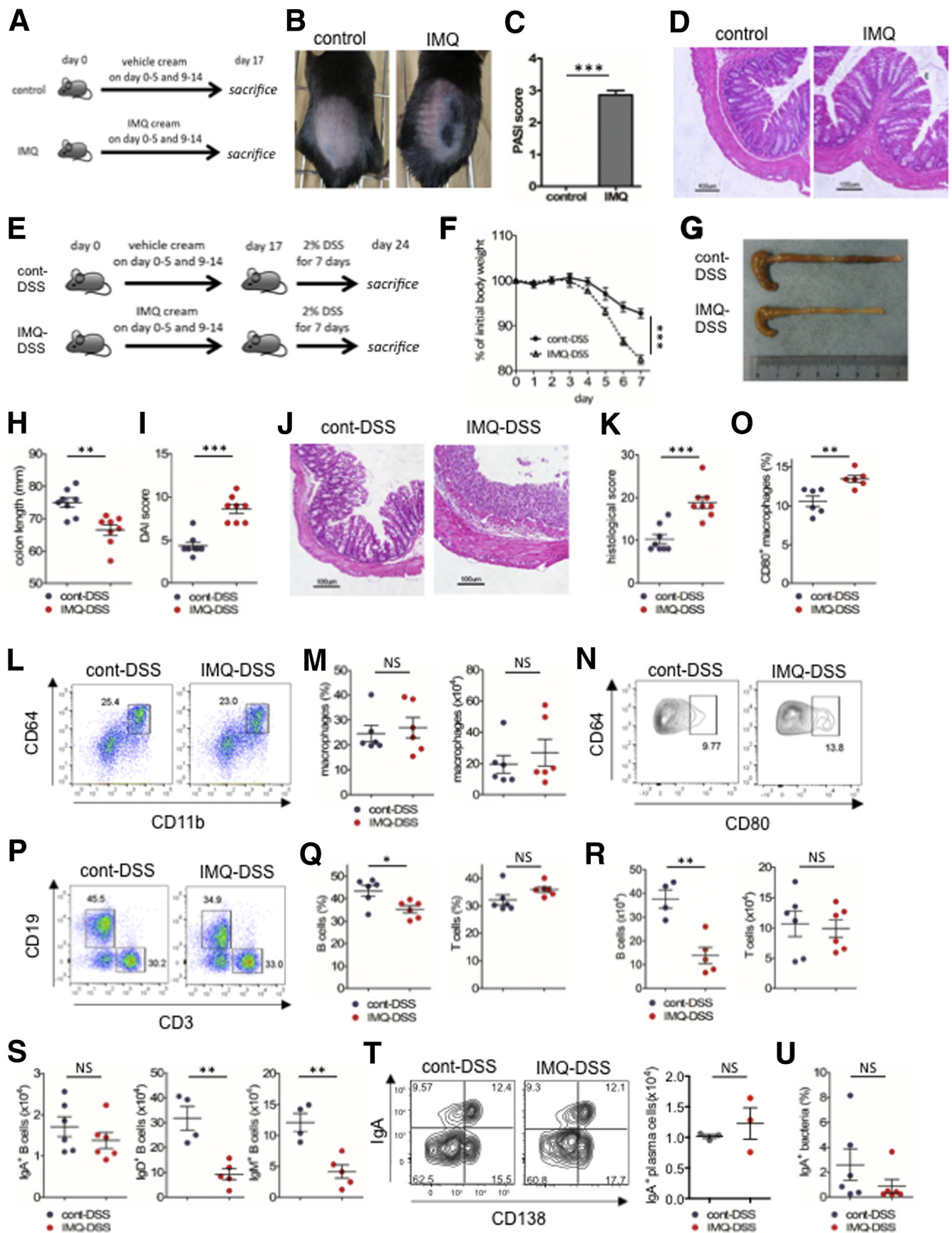
**Abbreviations used in this paper:** Abx, antibiotics; BM, bone marrow; BSA, bovine serum albumin; DAI, disease activity index; dLN, draining lymph node; DSS, dextran sulfate sodium; FITC, fluorescein isothiocyanate; GF, germ-free; gnoto, gnotobiot; HBSS, Hank's balanced salt solution; IBD, inflammatory bowel disease; IFN, interferon; IL, interleukin; ILC, innate lymphoid cell; IMQ, imiquimod; IP, intraperitoneally; IQI, IQI/Jic; LP, lamina propria; NLRP3, NACHT, LRR, and PYD domains-containing protein 3; OTU, operational taxonomic unit; PBS, phosphate-buffered saline; PCR, polymerase chain reaction; pDC, plasmacytoid dendritic cell; PE, phycoerythrin; PMA, phorbol 12-myristate-13-acetate; rRNA, ribosomal RNA; SPF, specific pathogen-free; Th, T helper; TLR, Toll-like receptor; TNF, tumor necrosis factor; Treg, regulatory T cells; WT, wild-type; ZO-1, zonula occludens-1.

 Most current article

© 2019 The Authors. Published by Elsevier Inc. on behalf of the AGA Institute. This is an open access article under the CC BY-NC-ND license (<http://creativecommons.org/licenses/by-nc-nd/4.0/>).

2352-345X

<https://doi.org/10.1016/j.jcmgh.2018.09.010>





IMQ-DSS mice compared with cont-DSS mice, whereas the numbers of IgA<sup>+</sup> B cells and IgA<sup>+</sup> plasma cells were not significantly different between the 2 groups (Figure 1S and T). Co-staining with antibodies against fecal bacteria and IgA showed that the proportion of fecal bacteria coated with secretory IgA was comparable in IMQ-DSS and cont-DSS mice (Figure 1U). These data indicate that IMQ dermatitis induced severe DSS colitis as well as decreased numbers of naive B cells and increased numbers of M1 macrophages in the gut.

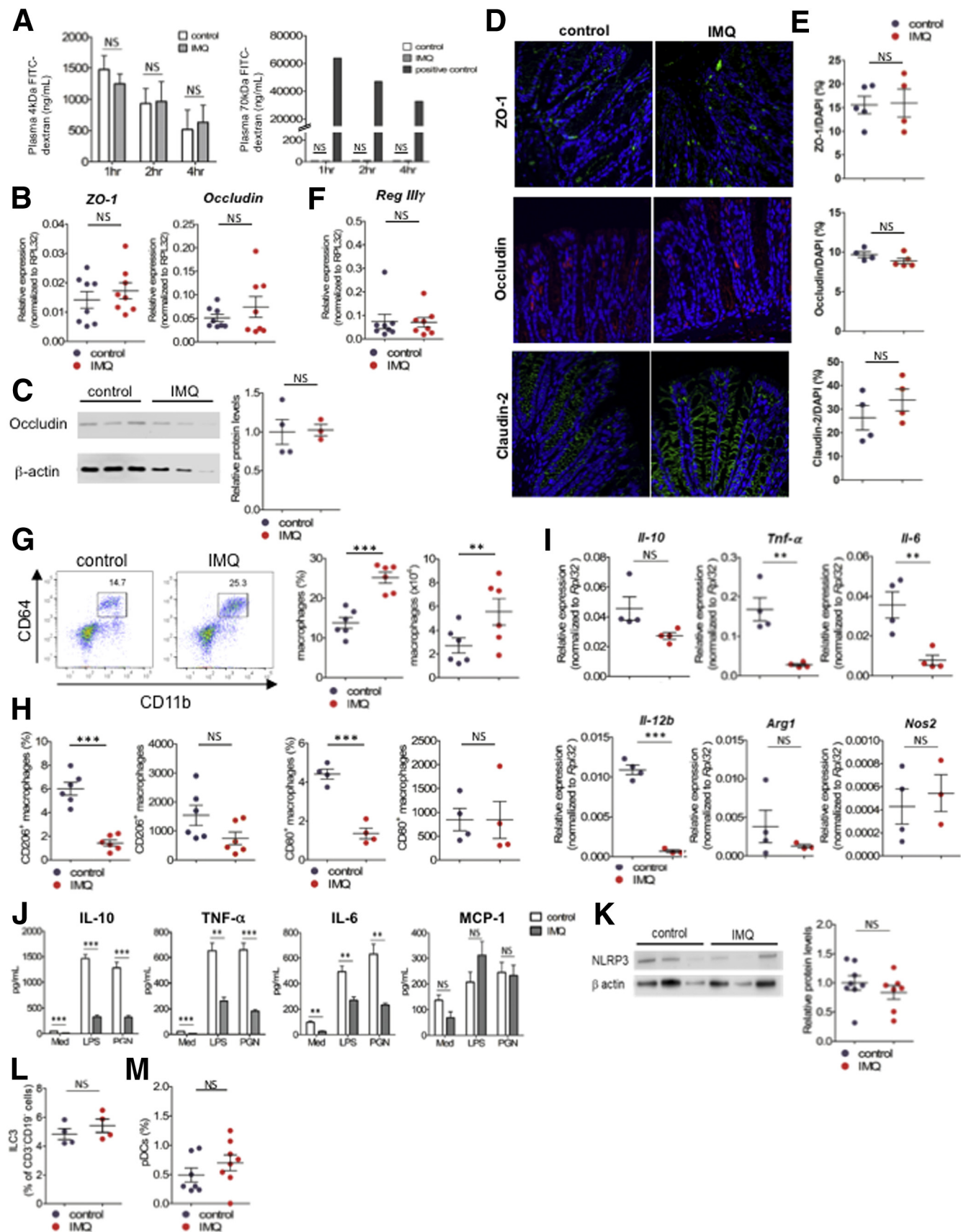
### IMQ Dermatitis Mice Did Not Increase Intestinal Permeability but Altered Immune Cell Composition in the Intestine

We next determined whether intestinal permeability and immunologic changes occurred in these animals before DSS challenge. To assess intestinal permeability, we administered 4 or 70 kilodaltons of fluorescein isothiocyanate (FITC)-dextran to fasting mice by oral gavage and analyzed plasma concentrations of FITC-dextran. Plasma levels of FITC-dextran were comparable in IMQ and control mice (Figure 2A). We also confirmed that expression of transcripts encoding the tight junction-associated proteins, zonula occludens-1 (ZO-1) and occludin, were not decreased in IMQ mice (Figure 2B). Western blot analysis of epithelial cells in IMQ mice showed occludin protein was not decreased (Figure 2C). Immunofluorescence staining of ZO-1, occludin, and claudin-2 were not decreased in colons of IMQ mice (Figure 2D and E). These data suggest that intestinal permeability was not increased in IMQ mice. We also confirmed that the expression of transcripts encoding the antimicrobial peptide Reg III $\gamma$  was not decreased in IMQ mice (Figure 2F). We observed that macrophage frequency in the gut was increased in IMQ mice (Figure 2G). Although the proportions of M1 (CD80<sup>+</sup>) and M2 (CD206<sup>+</sup>) macrophages were decreased in IMQ mice compared with control mice (Figure 2H), the absolute numbers of these cells were comparable. We next compared messenger RNA expression of CD11b<sup>+</sup> cells derived from colonic lamina propria (LP) (CD11b<sup>+</sup> cells) of IMQ and control mice. The relative expression of transcripts encoding proinflammatory cytokines such as tumor necrosis factor (TNF)- $\alpha$ , IL6, and IL12B

was reduced significantly in IMQ mice. Expression of IL10, an anti-inflammatory cytokine, was also slightly decreased, but this was not statistically significant ( $P = .063$ ) (Figure 2J). Expression of *Nos2* and *Arg1* were not different between the 2 groups. We collected LP CD11b<sup>+</sup> cells from IMQ and control mice and cultured them in vitro in the presence of lipopolysaccharide or peptidoglycan. Production of macrophage chemoattractant protein-1 by LP CD11b<sup>+</sup> cells was comparable between IMQ and control mice, whereas production of IL10, TNF- $\alpha$ , and IL6 was decreased significantly in LP CD11b<sup>+</sup> cells derived from IMQ mice (Figure 2J). Collectively, these data suggest that IMQ dermatitis increased the frequency of intestinal macrophages, but that these macrophages were impaired in their ability to produce both proinflammatory and anti-inflammatory cytokines (TNF- $\alpha$ , IL6, and IL10) against pathogen-associated molecular patterns. Because previous studies have shown that IMQ could activate the NACHT, LRR, and PYD domains-containing protein 3 (NLRP3) inflammasome in macrophages,<sup>17</sup> we analyzed NLRP3 expression in peritoneal cavity cells. However, NLRP3 expression in peritoneal cells was unaltered in IMQ mice (Figure 2K). IMQ is known to affect pDC and ILC3 populations,<sup>13</sup> but the proportions of pDCs and ILC3s were unaltered in IMQ mice compared with control animals (Figure 2L and M).

We next investigated the proportions of Th1 and Th17 cells and Tregs in colonic lamina propria, but did not find any differences between IMQ and control mice (Figure 3A, B, and D–G). Meanwhile, the number of colonic B cells was decreased drastically in IMQ mice (Figure 3A and C), mainly owing to reductions in IgD<sup>+</sup> and IgM<sup>+</sup> B cells not in IgA<sup>+</sup> B cells (Figure 3H). The percentage of plasma cells was not decreased before DSS administration to IMQ mice (Figure 3I). Because the amount of fecal IgA is known to affect dysbiosis, we also analyzed the concentration of secretory IgA and the proportion of IgA-coated bacteria in feces. Fecal IgA and IgA-coated bacteria levels were unaltered in IMQ mice, as we expected (Figure 3J and K). Taken together, IMQ mice did not increase intestinal permeability. IMQ mice reduced the number of IgD<sup>+</sup> and IgM<sup>+</sup> B cells and increased the number of macrophages that were impaired in their ability to produce cytokines in the gut before DSS administration.

**Figure 1. (See previous page). Psoriasis-like dermatitis exacerbates DSS colitis.** (A) Experimental protocol for induction of psoriasis-like dermatitis by IMQ. (B) Skin appearance of psoriasis-like dermatitis on day 14 of IMQ or vehicle treatment. (C) Clinical score for psoriasis-like dermatitis (psoriasis area severity index [PASI] score) at the end of IMQ treatment (on day 17). (D) Representative H&E staining of colon sections at the end of IMQ treatment (on day 17). Scale bar: 100  $\mu$ m. (E) Experimental protocol. Mice treated topically with IMQ or vehicle as shown in panel A, were subsequently induced with acute colitis by 2% (wt/vol) DSS for 7 days ( $n = 8$  in each group). (F) Body weight changes during administration of DSS. (G) Representative photograph of colon on day 7 of DSS colitis. (H) Colon length on day 7 of DSS colitis. (I) DAI score on day 7 of DSS colitis. (J) Representative H&E staining of distal colon section on day 7 of DSS colitis. Scale bar: 100  $\mu$ m. (K) Histologic score for colitis on day 7 of DSS colitis. (L) Representative plots of flow cytometry analysis for colonic lamina propria macrophages (CD45<sup>+</sup> lineage<sup>-</sup>CD11b<sup>+</sup>CD64<sup>+</sup> cells). The plots are gated on CD45<sup>+</sup>CD3<sup>-</sup>CD19<sup>-</sup>B220<sup>-</sup>NK1.1<sup>-</sup> cells. (M) Percentage (left) and absolute number (right) of colonic lamina propria macrophages. (N and O) Representative plots of flow cytometry analysis for CD80<sup>+</sup> macrophages in colonic lamina propria. Percentage of CD80<sup>+</sup> cells in macrophages. (P) Representative plots of flow cytometry analysis for CD45<sup>+</sup> colonic lamina propria lymphocytes. (Q and R) Percentage and absolute number of B cells (left) and T cells (right) in CD45<sup>+</sup> cells. (S) Absolute number of IgA<sup>+</sup> B cells (left), IgD<sup>+</sup> B cells (middle), and IgM<sup>+</sup> B cells (right). (T) Representative plots of flow cytometry analysis for IgA<sup>+</sup> plasma cells in colonic lamina propria (left) and absolute number (right). The plots are gated on CD45<sup>+</sup>CD3<sup>-</sup>CD4<sup>-</sup>CD8<sup>-</sup>NK1.1<sup>-</sup> cells. (U) Percentage of IgA-coated fecal bacteria analyzed by flow cytometry. Each symbol represents an individual mouse ( $n = 3$ –8). Statistical analyses were performed with the Student *t* test. \* $P < .05$ , \*\* $P < .01$ , \*\*\* $P < .001$ , NS; not significant. Error bars represent the SEM of samples within a group.



### Reduction of IgD<sup>+</sup> and IgM<sup>+</sup> B Cells Was Not Caused by Migration to Skin or Skin-Draining Lymph Nodes, or by Systemic B-Cell Depletion

We then hypothesized that IMQ dermatitis might cause gut-naive B cells to migrate to skin lesions or skin draining lymph nodes (dLNs). We analyzed the immune cell composition of both the dermis and epidermis of lesions as well as skin dLNs after IMQ application. The ratio of B cells was comparable in the dermis and epidermis of IMQ and control mice (Figure 3L–N). Similarly, the frequency of B cells was unaltered in skin dLNs of IMQ mice (Figure 3L–N). By contrast, as we previously found in the colon, the total numbers of B cells, IgD<sup>+</sup> B cells, and IgM<sup>+</sup> B cells were decreased in mesenteric lymph nodes of IMQ mice compared with control mice. To exclude the possibility of systemic B-cell reduction in IMQ mice, we analyzed splenic B cells and confirmed that splenic B cells were not decreased by IMQ application (Figure 3L and M). We also analyzed Th17 cells, Th1 cells, and Tregs in each organ. Both Tregs and Th17 cells were increased in skin dLNs and mesenteric lymph nodes. Th1 cells were slightly increased in skin dLNs. However, the ratio of Th17, Th1, and Tregs did not increase in the colons of IMQ mice (Figure 3D–G). These data indicate that colonic IgD<sup>+</sup> and IgM<sup>+</sup> B cells in IMQ mice did not migrate to skin or skin dLNs.

### Psoriasis-Like Dermatitis Was Required to Induce Immunologic Changes in the Gut and to Exacerbate DSS Colitis

We next assessed whether psoriasis-like dermatitis was required for immunologic changes and severe colitis to occur in the gut after IMQ treatment. First, we applied IMQ to TLR7<sup>-/-</sup> mice (IMQ-ΔTLR7) to determine whether

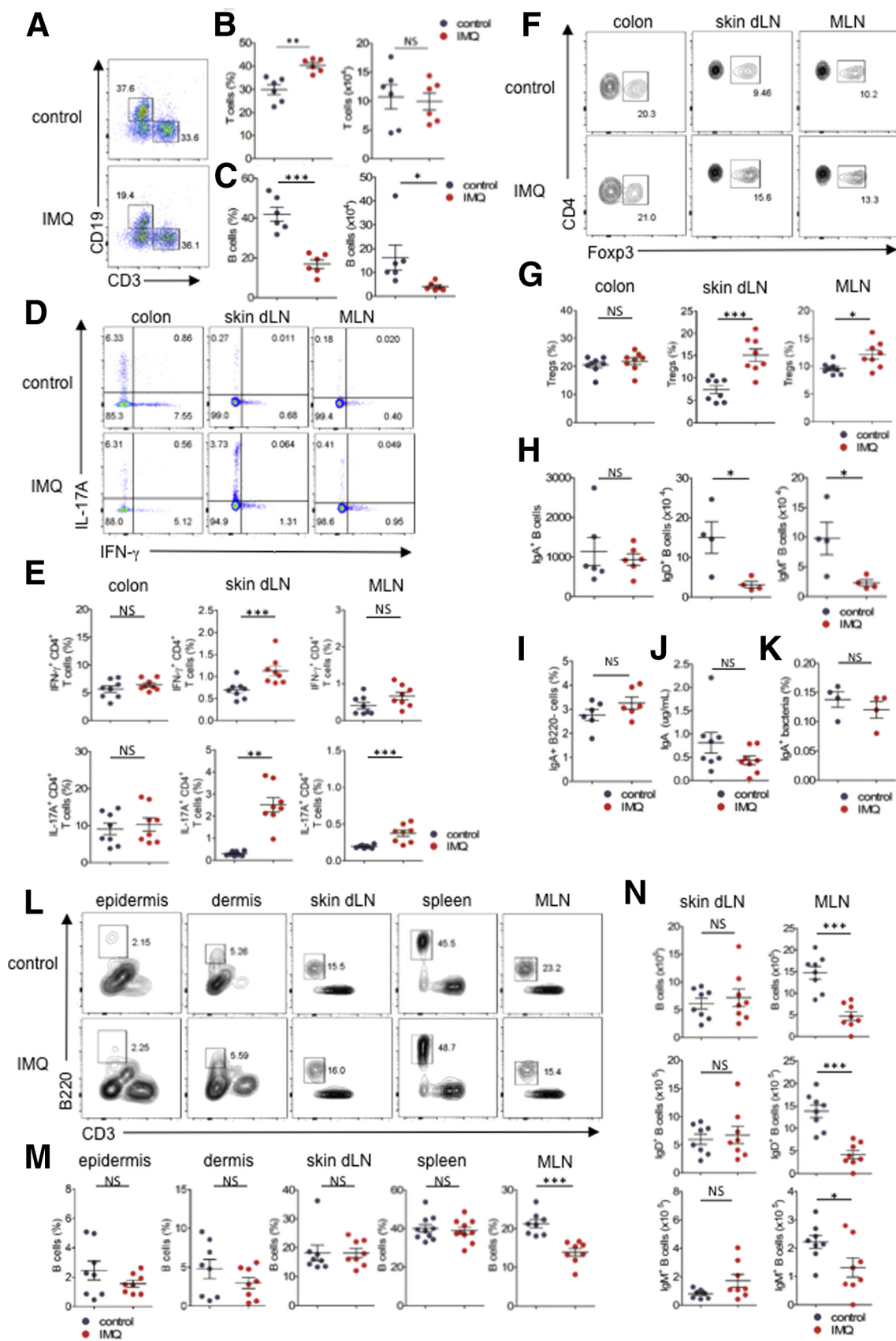
naive B-cell reduction in the gut was TLR7-dependent. IMQ-ΔTLR7 mice showed mild dermatitis compared with control mice (Figure 4A and B), but showed no evidence of gut B-cell reduction (Figure 4C). Thus, naive B-cell reduction after IMQ treatment was TLR7-dependent, although it is possible that the severity of dermatitis might impact the magnitude of naive B-cell reductions in the gut. It has been reported that mice treated with a combination of TLR3 and TLR7 agonists show ameliorated DSS colitis because of reduced TNF-α production by CD11b<sup>+</sup> macrophages.<sup>12</sup> To explore the effects of route of administration, we treated the mice with IMQ or phosphate-buffered saline (PBS) via intraperitoneal (IP) injection (IMQ IP mice and PBS IP mice, respectively) (Figure 4D). We observed increased absolute numbers of macrophages and T cells in IMQ IP mice, as previously reported (Figure 4E–G). However, B cells were not decreased in IMQ IP mice (Figure 4H and J). We then administered 2% (wt/vol) DSS to IMQ IP and PBS IP mice (IMQ IP–DSS mice and PBS IP–DSS mice, respectively) (Figure 4J). IMQ IP–DSS mice did not ameliorate colitis compared with PBS IP–DSS mice (Figure 4K–N). Thus, development of dermatitis was indispensable to recapitulate the phenotype of exacerbated DSS-induced colitis after IMQ treatment.

### IMQ Dermatitis Altered Gut Microbial Composition

It is well known that microbes and the immune system interact with one another. For instance, some *Clostridium* species induce Treg differentiation via short-chain fatty acids, and secretory IgA coats fecal *Escherichia coli* in patients with Crohn's disease.<sup>18</sup> It was reported previously that the microbiome composition in IBD patients was similar to that of psoriasis patients.<sup>10,11</sup> We hypothesized that the microbiome composition of IMQ mice might differ from control mice, and so we subjected fecal samples from

**Figure 2. (See previous page). IMQ dermatitis mice did not increase intestinal permeability but altered immune cell composition in the intestine.** (A) Analysis for intestinal permeability of mice induced psoriasis-like dermatitis (on day 17 of IMQ or vehicle treatment), by using 4 kilodaltons (left) or 70 kilodaltons (right) FITC-dextran. Plasma FITC-dextran concentrations were determined by fluorescence intensity, after 1, 2 and 4 hours from oral administration of FITC-dextran (n = 4, in each group). Seventy kilodaltons FITC-dextran was administered intravenously as a positive control. (B) Quantitative PCR analysis for ZO-1 and occludin in colonic epithelial cells after topical IMQ treatment (on day 17) analyzed by real-time PCR. (C) Western blot analysis for occludin expression in colonic epithelial cells after topical IMQ treatment (on day 17). Western blot (left) and relative protein levels (right) of occludin. (D) Immunofluorescence staining was performed in control and IMQ mice. ZO-1 (top, green), occludin (middle, red), claudin (bottom, green) stained with 4',6-diamidino-2-phenylindole (DAPI; blue) in colon tissue. Four to 5 sections from each mice were obtained and the average positive area of each protein was compared with the DAPI-positive area measured (n = 4–5, each dot represents each mouse). (E) Quantitative PCR analysis for *Reg IIIγ* in colonic epithelial cells after topical IMQ treatment (on day 17) analyzed by real-time PCR. (F) Representative plots of flow cytometry analysis for macrophages (CD11b<sup>+</sup>CD64<sup>+</sup> cells) in CD45<sup>+</sup>CD3<sup>-</sup>CD19<sup>-</sup>B220<sup>-</sup>NK1.1<sup>-</sup> colonic lamina propria after IMQ treatment (on day 17) (n = 6 in each group). Percentage (left) and absolute number (right) of macrophages in colonic lamina propria. (H and I) Percentage and absolute number of CD206<sup>+</sup> (left) or CD80<sup>+</sup> (right) macrophages. (J) Quantitative PCR analysis of *IL10*, *Tnf-α*, *Il6*, *IL12b*, *Arg-1*, and *Nos2* in LP CD11b<sup>+</sup>s (n = 3–4 in each group). (K) CD11b<sup>+</sup> cells were sorted by magnetic activated cell sorting from colonic lamina propria mononuclear cells on day 17 of IMQ treatment (LP CD11b<sup>+</sup>s). LP CD11b<sup>+</sup>s were cultured with lipopolysaccharide (LPS) or peptidoglycan (PGN) for 24 hours in vitro, and concentrations of cytokines in the supernatant were measured by cytometric bead array. Unstimulated control was cultured with medium (Med). (L) Western blot analysis for NLRP3 in peritoneal cavity cells, which are composed mainly of macrophages. Western blot (left) and relative protein levels (right) of NLRP3 (n = 7–8, pooled from 2 independent experiments, in each group). (M) Percentage of ILC3 in CD45<sup>+</sup>CD3<sup>-</sup>CD19<sup>-</sup> cells and (N) pDCs in CD45<sup>+</sup>CD11b<sup>-</sup>CD11c<sup>+</sup> cells in colonic lamina propria (ILC3, CD45<sup>+</sup>CD3<sup>-</sup>CD19<sup>-</sup>Roryt<sup>+</sup> cells; pDC, CD45<sup>+</sup>CD11b<sup>-</sup>CD11c<sup>+</sup>B220<sup>+</sup>PDCA-1<sup>+</sup> cells). Each symbol represents an individual mouse (n = 4–8). Statistical analyses were performed with the Student *t* test. \**P* < .05, \*\**P* < .01, \*\*\**P* < .001. Error bars represent the SEM of samples within a group.





both groups of mice to 16S ribosomal RNA (rRNA) metagenomic analysis. The number of operational taxonomic units (OTUs), as well as  $\alpha$  diversity measured using either the Chao1 index or the phylogenetic diversity whole tree metric, were comparable between the 2 groups (Figure 5A). As we expected, a principal coordinate analysis using the unweighted or weighted UniFrac distances between microbial communities showed that the microbial composition of IMQ mice was significantly different from control mice (Figure 5B). At the phylum level, *Firmicutes* populations were slightly decreased and *Bacteroidetes* populations were slightly increased in IMQ mice (Figure 5C). At the family level, *Lactobacillaceae* populations were reduced drastically in IMQ mice (Figure 5D and E), and both *Erysipelotrichaceae* and *Desulfovibrionaceae* populations were decreased to a lesser extent. At the genus level, we observed a drastic reduction in *Lactobacillus* populations in IMQ mice (Figure 5F–H), decreases in *Desulfovibrio* and *Allobaculum* populations, and an increase in *Dorea* populations. We concluded that psoriasis-like dermatitis altered the gut microbial composition of IMQ-treated mice.

### Gut Microbiomes in IMQ Mice Are Essential to Induce Severe DSS Colitis

Next, whether immunologic changes in IMQ mice were caused directly by IMQ-induced dermatitis or by gut dysbiosis, we applied either IMQ or vehicle alone to mice along with a mixture of 4 antibiotics (Abx) (ampicillin, neomycin, vancomycin, and metronidazole), targeting both gram-positive and gram-negative bacteria (Abx-IMQ mice and Abx-cont mice, respectively) (Figure 6A). Interestingly, the number of B cells in the colonic lamina propria, but not the number of macrophages, was reduced in Abx-IMQ mice compared with Abx-cont mice (Figure 6B–H). These results indicated that topical application of IMQ directly decreased B cells in the gut in a microbe-independent manner, whereas the increased number of macrophages might result from IMQ-induced dysbiosis. To further confirm the role of intestinal microbes in IMQ mice, we tested whether antibiotic therapy rescued the aggravation of colitis in IMQ-DSS mice. We administered either the 4-Abx mixture

mentioned earlier or distilled water 3 times a week by oral gavage to IMQ mice and control mice, starting 1 week before topical treatment. After topical treatment of IMQ or vehicle, 2% (wt/vol) DSS in drinking water was administered ad libitum to all mice. Abx or distilled water was administered until the end of the experiment (Figure 6J). We confirmed that the degree of psoriasis-like dermatitis was unaffected by treatment with Abx (Figure 6J). As expected, IMQ mice treated with Abx (Abx-IMQ-DSS) had ameliorated colitis compared with IMQ mice without Abx treatment (water-IMQ-DSS), including lesser body weight loss, longer colon lengths, lower DAI scores, and less severe histologic findings (Figure 6K–Q). The severity of colitis was comparable in Abx-IMQ-DSS and Abx-cont-DSS mice. Gut microbiomes have a crucial role to exacerbate IMQ-DSS colitis.

It remained unclear whether immune cells or gut microbes in IMQ mice were the direct mediator of severe DSS colitis. We hypothesized that dysbiosis in IMQ mice was essential for accelerated colitis. To test this hypothesis, we obtained fecal contents from control mice or IMQ mice and performed fecal transfers to GF IQI mice (cont gnotobiot [gnoto] mice and IMQ gnoto mice, respectively) in vinyl isolators (Figure 7A). IMQ gnoto mice did not develop spontaneous colitis (data not shown). We observed that the ratio of IgD<sup>+</sup> B cells in the gut of IMQ gnoto mice was slightly reduced compared with cont gnoto mice, but we observed no difference in macrophages and B-cell numbers between these groups (Figure 7B–D). We then fed DSS in drinking water to these mice 3 weeks after fecal transplantation (Figure 7E). Mice transplanted with feces from IMQ mice and treated with DSS (IMQ gnoto-DSS mice) showed more severe clinical symptoms than mice transplanted with control mouse feces (cont gnoto-DSS mice), including lower body weight, shorter colon length, loose stool consistency, and gross bleeding. This was reflected in the higher partial DAI scores of these animals (Figure 7F–I). Histologic analysis of colons of IMQ gnoto-DSS mice showed more severe destruction of epithelial integrity, loss of crypts, submucosal edema, and higher intestinal inflammation with immune cell infiltrates; this was reflected by higher histologic scores in these animals

**Figure 3.** (See previous page). The reduction of IgD<sup>+</sup> and IgM<sup>+</sup> B cells of colon in IMQ mice was not caused by migration to skin or skin draining lymph nodes, or by systemic B-cell depletion. (A) Representative plots of flow cytometry analysis for lymphocytes in CD45<sup>+</sup> colonic lamina propria. (B and C) Percentage (left) and absolute number (right) of (B) T cells and (C) B cells in CD45<sup>+</sup> colonic lamina propria as shown in panel A. (D) Representative plots of flow cytometry analysis for IFN- $\gamma$  and IL17A in CD3<sup>+</sup>CD4<sup>+</sup> cells from colonic lamina propria, skin dLN, and mesenteric lymph node (MLN), stimulated with PMA, ionomycin, and IL23 for 4 hours. (E) Percentage of IFN- $\gamma$ <sup>+</sup> (top) and IL17A<sup>+</sup> (bottom) cells in CD3<sup>+</sup>CD4<sup>+</sup> lymphocytes from each organ. (F and G) Intracellular staining and the ratio of Foxp3 in CD3<sup>+</sup>CD4<sup>+</sup> lymphocytes from each organ. (H) Absolute number of IgA<sup>+</sup> B cells (left), IgD<sup>+</sup> B cells (middle), and IgM<sup>+</sup> B cells (right). (I) Percentage in CD45<sup>+</sup> cells of IgA<sup>+</sup>B220<sup>-</sup> plasma cells. (J) Concentration of IgA in feces measured by enzyme-linked immunosorbent assay. (K) Percentage of IgA-coated bacteria in feces. (L) Representative plots of flow cytometry analysis for B cells in epidermis, dermis, skin dLNs, spleen, and MLN after topical IMQ treatment. The numbers within plots indicate the percentages of gated cells. The plots are gated on CD45<sup>+</sup> cells. (M) Percentages of B cells in CD45<sup>+</sup> cells in epidermis, dermis, skin dLN, spleen, and MLN as shown in panel L. (N) Absolute number of B cells (top), IgD<sup>+</sup> B cells (middle), and IgM<sup>+</sup> B cells (bottom) in skin dLN and MLN. Each symbol represents an individual mouse (n = 4–8). Statistical analyses were performed with the Student *t* test. \**P* < .05, \*\**P* < .01, \*\*\**P* < .001. Error bars represent the SEM of samples within a group.



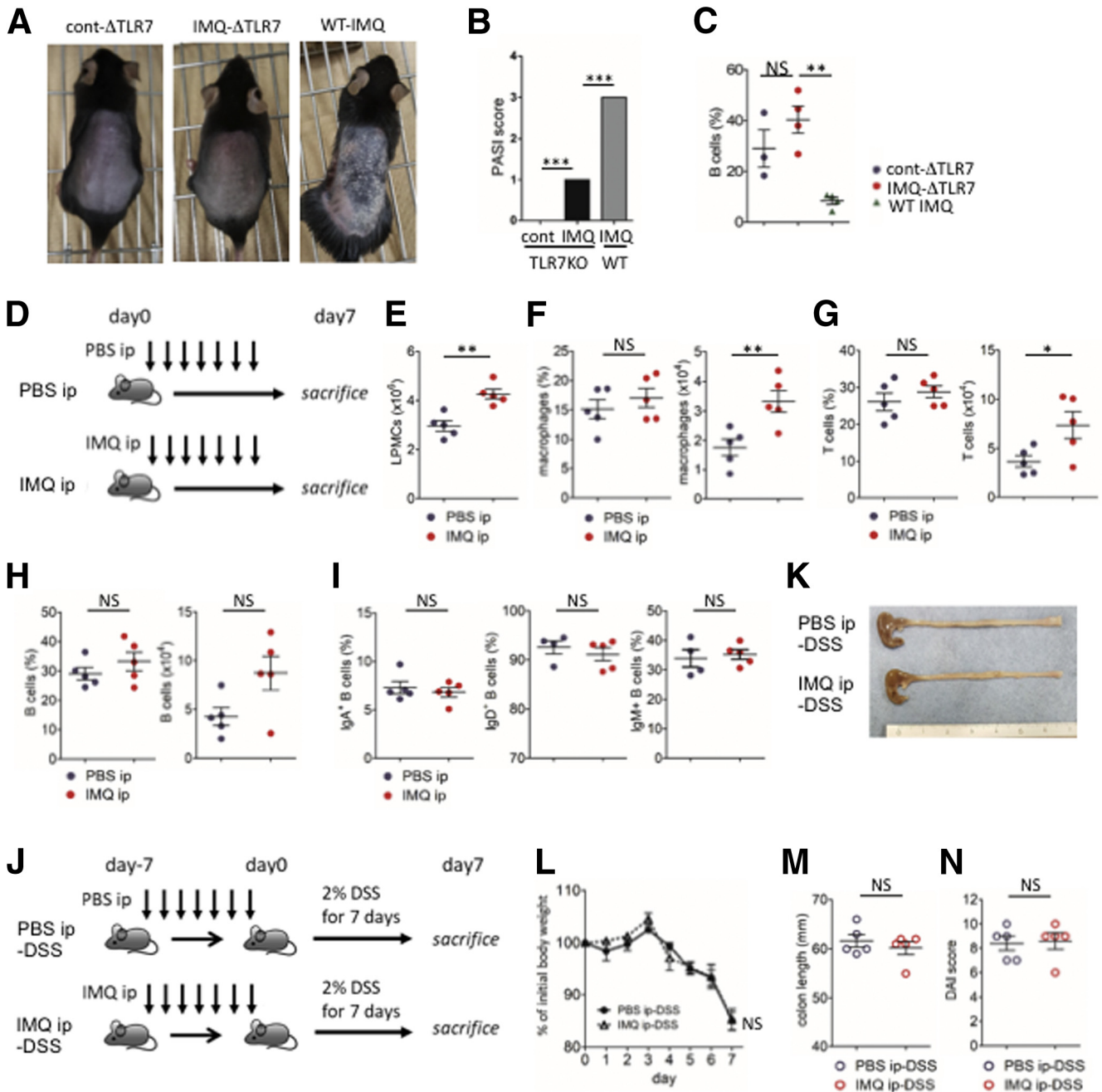
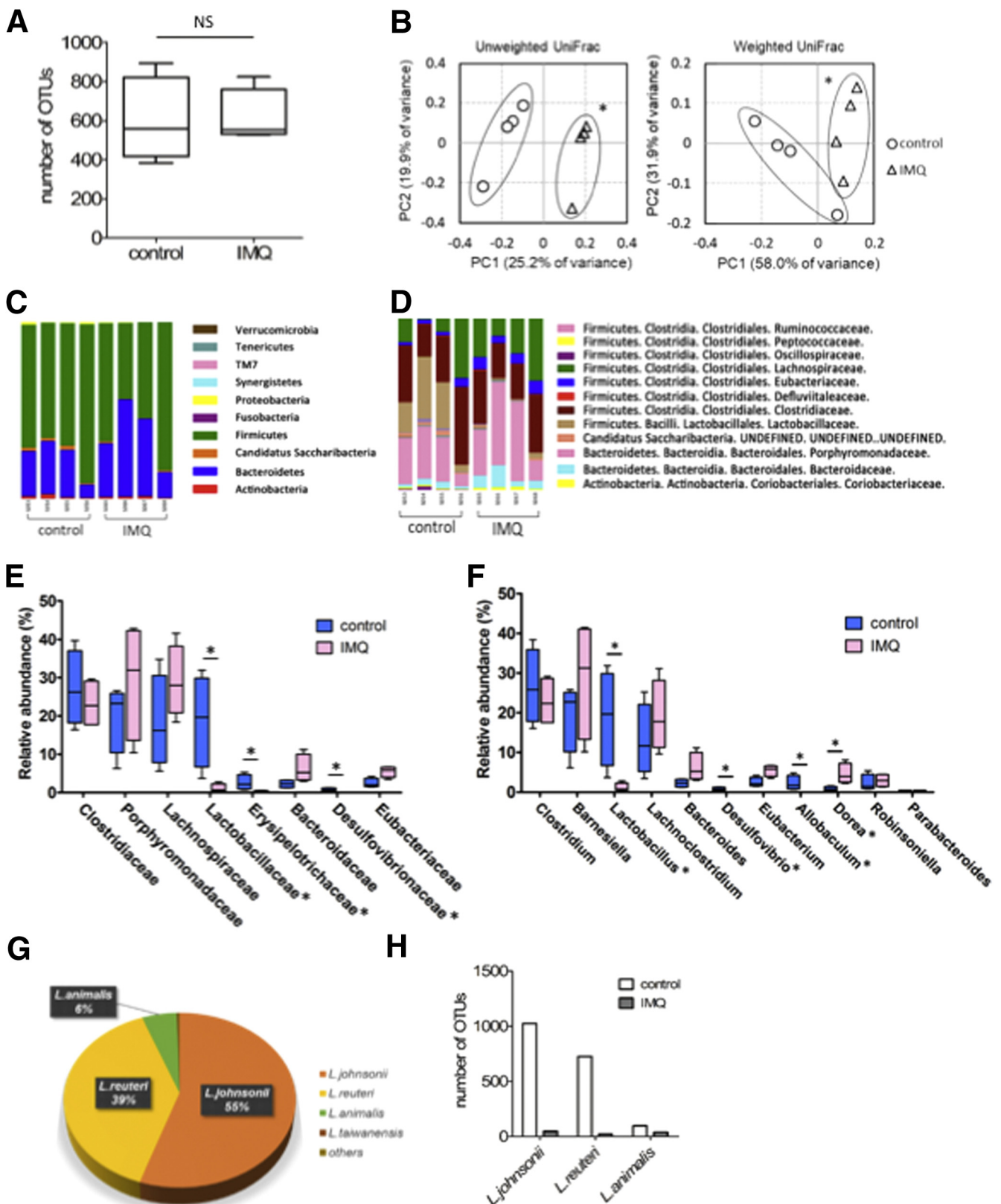


**Figure 4. Psoriasis-like dermatitis was required to induce immunologic changes in the gut and to exacerbate DSS colitis.** (A–C) Psoriasis-like dermatitis was induced by topical IMQ treatment in TLR7<sup>-/-</sup> mice (IMQ- $\Delta$ TLR7 mice) and WT mice (WT-IMQ mice). As control, vehicle was applied to TLR7<sup>-/-</sup> mice (cont- $\Delta$ TLR7 mice) instead of IMQ, and the severity of dermatitis and B cell change in colonic lamina propria were assessed. Skin appearance after induction of psoriasis-like dermatitis by (A) IMQ, (B) Psoriasis Area and Severity Index (PASI) score, and (C) the percentage of B cells in colonic lamina propria analyzed by flow cytometry. (D–I) IMQ was injected IP to mice daily for a week and lymphocytes in colonic lamina propria were analyzed. PBS was injected instead of IMQ as control. (D) Experimental protocol, (E) absolute number of lamina propria mononuclear cells (LPMCs), (F) percentage in CD45<sup>+</sup> lineage<sup>-</sup> cells (left) and absolute number (right) of macrophages in colonic lamina propria, (G) percentage in CD45<sup>+</sup> cells (left) and absolute number (right) of T cells, and (H) B cells. (I) Percentages in the total B cells of IgA<sup>+</sup> B cells, IgD<sup>+</sup> B cells, and IgM<sup>+</sup> B cells. (J) Experimental protocol. Mice injected IP with IMQ or PBS were further administered 2% (wt/vol) DSS for 7 days to induce colitis, and the severity of colitis was assessed. (K) Representative photograph of colon on day 7 of DSS colitis. (L) Body weight change during DSS administration. (M) Colon length on day 7 of DSS colitis. (N) DAI score on day 7 of DSS colitis. Each symbol represents an individual mouse (n = 3–5). Statistical analyses were performed with the Student *t* test. \**P* < .05, \*\**P* < .01, \*\*\**P* < .005. Error bars represent the SEM of samples within a group. Lineage, CD3, CD19, B220, and NK1.1.

than in cont gnoto-DSS mice (Figure 7J and K). These results indicate that the gut microbiomes of IMQ mice had the potential to accelerate gut inflammation in the DSS

colitis model. Based on these results, in concert with our previous data, we concluded that dysbiosis in IMQ mice was essential to accelerate DSS colitis.



### Neither Administration of *Lactobacillus* Strains nor Fecal Transplantation Ameliorated Colitis in IMQ-DSS Mice

We previously showed that dysbiosis in IMQ mice caused more severe DSS-induced colitis. We next considered whether microbiome alterations might be therapeutic for IMQ mice. We transplanted the fecal contents of WT mice to IMQ mice and fed them 2% DSS in their drinking water (IMQ<sub>[wild-type (WT) fecal microbe transplantation (FMT)]</sub>-DSS mice) (Figure 7L). IMQ<sub>(WT FMT)</sub>-DSS mice and IMQ-DSS mice developed comparably severe colitis (Figure 7M–O). We further analyzed the effects of specific bacterial strains on IMQ-DSS mice. Because we had observed large reductions of *Lactobacillus* populations in IMQ mice, we focused on *Lactobacillus* species. Three major species of *Lactobacillus* were detected in the feces of control mice. *Lactobacillus johnsonii* and *Lactobacillus reuteri* made up approximately 55% and 40% of all *Lactobacillus* species in control mice, respectively (Figure 5G). We confirmed that those 2 species were greatly reduced in the feces of IMQ mice (Figure 5H). Several *Lactobacillus* species, including *L. johnsonii* and *L. reuteri*, have been reported to have protective roles in intestinal inflammation.<sup>19–26</sup> We inoculated either a cocktail of *L. johnsonii* and *L. reuteri* or water to IMQ mice during DSS treatment (IMQ<sub>[Lacto]</sub>-DSS mice or IMQ<sub>[water]</sub>-DSS mice, respectively) (Figure 7P). IMQ<sub>(Lacto)</sub>-DSS mice did not show ameliorated colitis compared with IMQ<sub>(water)</sub>-DSS mice (Figure 7Q–S). Thus, although antibiotic therapy could rescue IMQ-DSS colitis (Figure 6I–Q) and intestinal dysbiosis mediated the exacerbation of DSS-induced colitis, neither fecal transplantation nor treatment with cocktails of *L. johnsonii* and *L. reuteri* ameliorated DSS colitis in IMQ mice.

### Both Hematopoietic and Nonhematopoietic TLR7-Positive Cells Enhance IMQ-DSS Colitis

We further analyzed whether hematopoietic or non-hematopoietic cells were essential for IMQ-DSS colitis. After irradiation to WT mice, we injected bone marrow cells obtained from WT or TLR7<sup>-/-</sup> mice (WT<sup>bone marrow[BM]</sup>/ΔTLR7<sup>BM</sup>). After 6 weeks of bone marrow transplantation, we applied vehicle or IMQ (WT<sup>BM</sup>/ΔTLR7<sup>BM</sup>/WT<sup>BM</sup>-IMQ/ΔTLR7<sup>BM</sup>-IMQ mice, respectively) (Figure 8A). We observed ΔTLR7<sup>BM</sup>-IMQ mice induce dermatitis as well as WT<sup>BM</sup>-IMQ mice (data not shown). Then, we inoculated 2% (wt/vol) DSS to each group of mice (WT<sup>BM</sup>-DSS/ΔTLR7<sup>BM</sup>-DSS/WT<sup>BM</sup>-IMQ-DSS/ΔTLR7<sup>BM</sup>-IMQ-DSS mice, respectively). Both IMQ dermatitis groups, WT<sup>BM</sup>-IMQ-DSS and ΔTLR7<sup>BM</sup>-IMQ-DSS mice exacerbated colitis compared with WT<sup>BM</sup>-DSS

mice or ΔTLR7<sup>BM</sup>-DSS mice, respectively, in body weight loss, colon length, and DAI (Figure 8B–F). We also confirmed that ΔTLR7<sup>BM</sup>-IMQ-DSS mice had an increased histologic score compared with ΔTLR7<sup>BM</sup>-DSS mice (Figure 8G and H). These data showed that nonhematopoietic resident cells that expressed TLR7 were responsible for the IMQ dermatitis-DSS colitis model. Because ΔTLR7<sup>BM</sup>-DSS mice ameliorated colitis compared with WT<sup>BM</sup>-DSS mice, TLR7-positive hematopoietic cells also were involved in the IMQ-colitis model.

## Discussion

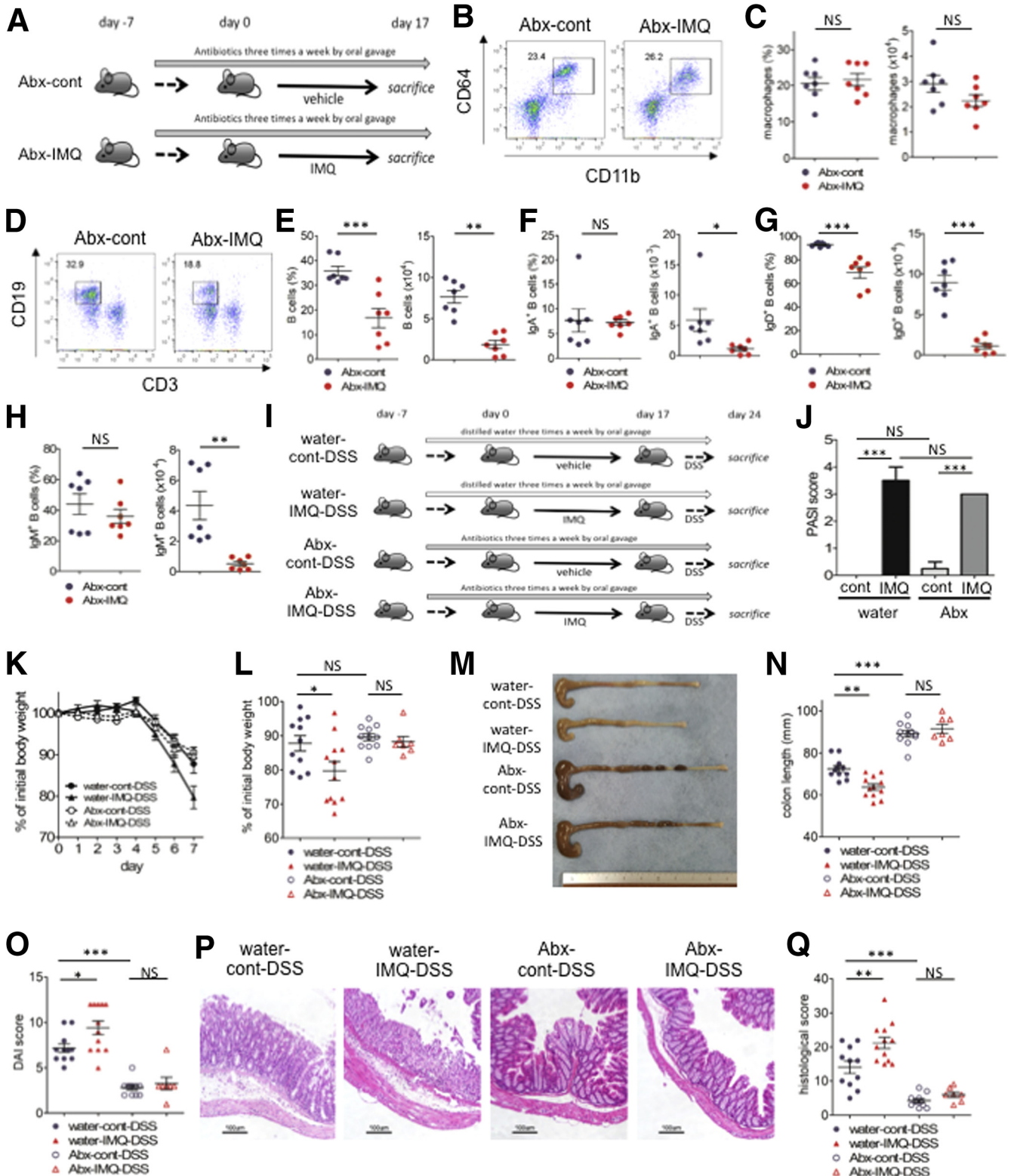
IBD and psoriasis are different diseases, involving chronic inflammatory conditions in the gut and skin, respectively. These conditions share several similarities, both involving commensal microbial communities and potential immune mechanisms. However, little is known regarding potential mechanisms of interaction between dermatitis and colitis. In this study, we first showed that psoriasis-like dermatitis triggered by a TLR7 agonist (IMQ) exacerbated DSS-induced colitis. Second, we found that IMQ dermatitis resulted in reduced numbers of IgD<sup>+</sup> and IgM<sup>+</sup> B-cell numbers and increased numbers of nonfunctional macrophages in the gut. Third, we showed that IMQ dermatitis caused dysbiosis, which mediated accelerated DSS colitis. The results of our study support the existence of a skin–gut axis: skin inflammation fosters proinflammatory conditions in the gut, resulting in dysbiosis and B-cell reductions. Our study's first major result was the observation that IMQ-induced psoriasis-like dermatitis affected gut immune cell composition. IMQ mice had dramatically reduced IgD<sup>+</sup> and IgM<sup>+</sup> B cells and increased numbers of macrophages that were impaired in their ability to produce cytokines. The increase in macrophage number was abrogated in antibiotic-treated mice, suggesting that intestinal microbes in IMQ mice were involved in increasing macrophage frequency. We then showed that IMQ dermatitis decreased IgD<sup>+</sup> and IgM<sup>+</sup> B cells in a microbe-independent manner. Interestingly, decreased numbers of IgD<sup>+</sup> and IgM<sup>+</sup> B cells were not observed when IMQ was administered IP. This suggests that IMQ dermatitis, but not IMQ itself, was essential to reduce B cells in the gut. Other groups also have reported that IgM-positive B cells were indispensable to protect against DSS colitis in MyD88 knockout (KO) mice.<sup>27</sup> B-cell intrinsic MyD88 signaling had a key role in the resistance to DSS via the production of IgM. These data support our findings that a massive reduction of IgM<sup>+</sup> B cells in IMQ mice induced severe DSS colitis. Further

**Figure 5.** (See previous page). IMQ-induced psoriasis-like dermatitis alters gut microbial compositions. 16S rRNA metagenomic analysis for fecal samples derived from mice after IMQ or vehicle treatment (n = 4 in each group). Feces were collected on day 17 of IMQ or vehicle treatment, as shown in Figure 1A. (A) Number of OTUs. (B) Principal coordinate analysis based on unweighted UniFrac distances (left) and weighted UniFrac distances (right). The 2 principal components (PC1 and PC2) explained 45.1% and 89.9% in the principal coordinate analysis based on unweighted and weighted UniFrac distances, respectively. (C) Phylum and (D) family level bacterial compositions of IMQ or vehicle-treated mice. (E and F) Relative abundance of each (E) family and (F) genera. (G) Proportion of each *Lactobacillus* species in control mice. (H) Relative abundance of 3 dominant *Lactobacillus* species in control and IMQ mice. Statistical analyses were performed with (A, E, and F) the Mann–Whitney U test, or (B) the Permanova test. \*P < .05. Error bars represent the SEM of samples within a group.



studies are needed to show how dermatitis might result in a reduction of IgD<sup>+</sup> and IgM<sup>+</sup> B cells in the gut. There are 2 obvious possibilities. One possibility involves IMQ triggering systemic inflammation through the lymphatic vessels or

blood stream. Body weight is reduced transiently during the first few days after topical IMQ application. However, the frequencies of macrophages and B cells in the spleen were not altered in IMQ mice. We confirmed that B cells did not



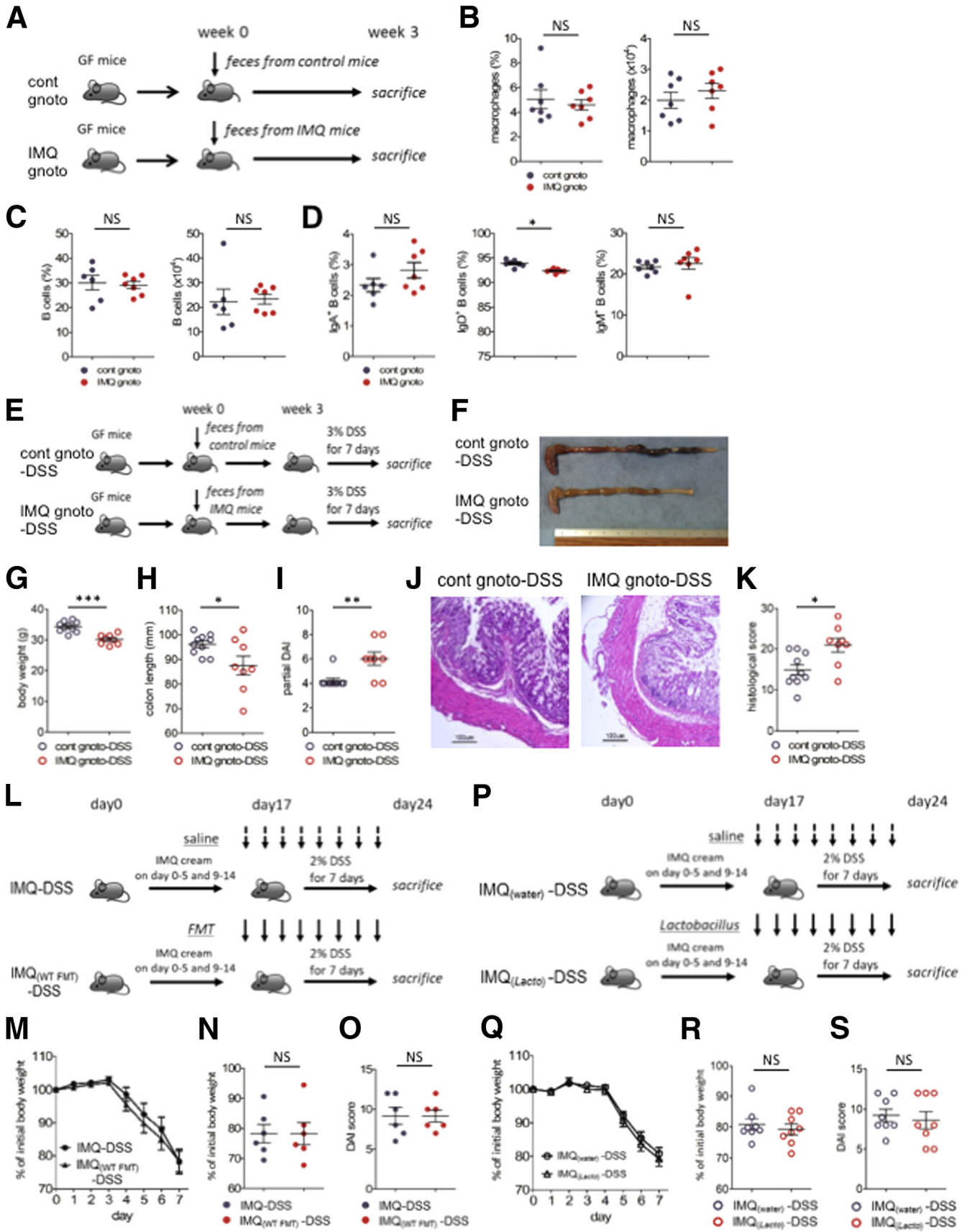
accumulate in skin and skin draining lymph nodes after IMQ treatment, suggesting that B cells in the gut of IMQ mice might not move to other organs. It previously has been reported that systemic administration of TLR3 and TLR7 agonists ameliorated colitis through enhanced production of IFN- $\beta$  by activated pDCs upon TLR7 signaling.<sup>12</sup> In contrast to the previous report, the number of pDCs in the gut of IMQ mice was unaltered. This discrepancy might be related to the route of administration of IMQ (topical vs systemic). It is well known that there is a variety of TLR7-expressing cells, including B cells, pDCs, and c-fiber neurons. We also confirmed that  $\Delta$ TLR7<sup>BM</sup>-IMQ-DSS mice had severe colitis compared with  $\Delta$ TLR7<sup>BM</sup>-DSS mice. These data indicated that TLR7-expressed nonhematopoietic cells played significant roles in IMQ-DSS colitis. However,  $\Delta$ TLR7<sup>BM</sup>-DSS had less severe colitis compared with WT<sup>BM</sup>-DSS mice. It also suggested that TLR7-expressing hematopoietic cells also involved the skin-gut axis. According to the previous experiments, the other possibility is a potential neuro-immune interaction involving skin-affected gut sites. Recently, peripheral TRPV1<sup>+</sup>Na<sub>v</sub>1.8<sup>+</sup> nociceptive sensory neurons have been reported to interact with dermal dendritic cells, which are the principal source of IL23 in the skin, and this interaction was found to be essential for the development of psoriasis-like dermatitis in IMQ-induced models.<sup>28</sup> Nociceptors are associated not only with local skin inflammation, but transfer neurodamage signals to the brain as pain. It once was thought that cytokines produced by immune cells might induce sensory nerve activation and pain signaling; however, recent studies have shown that pathogens and neurodamage could directly activate nociceptors, and that TLRs were instrumental in bilateral interactions between neurons and immune cells. For instance, C fibers in the dermis are known to express TLR7<sup>29</sup> and TLR4. Nociceptors sense pathogens through TLR4, TLR7, and TRPV1.<sup>29-31</sup> Similar to dermal nerves, enteric neurons express TLR2 or TLR4,<sup>32</sup> and glial cells express TLR7.<sup>33</sup> Gut microbes alter the phenotypes of macrophages surrounding enteric neurons, and these macrophages directly regulate the activity of enteric neurons.<sup>34,35</sup> Further studies are needed to elucidate the precise

mechanisms of skin-brain-gut neuroimmune interactions. Again, our results did not deny the concomitance of TLR7-positive immune cells in the IMQ-DSS model because  $\Delta$ TLR7<sup>BM</sup>-DSS mice had less severe colitis compared with WT<sup>BM</sup>-DSS mice.

Our study's second major result was the demonstration that IMQ treatment of mice induced dysbiosis, especially marked reductions of *Lactobacillus* species, which mediated severe DSS colitis. We confirmed that total amounts of IgA in feces and gut were not altered by IMQ treatment. Both intestinal permeability and antimicrobial peptide production were unchanged in IMQ mice. Future studies will need to establish novel models to investigate connections between B-cell reduction or neural damage in the gut and dysbiosis. *L. johnsonii* is known to have a protective role in the 2,4,6-trinitrobenzene sulfonic acid colitis model.<sup>19,20</sup> However, administration of *Lactobacillus* species did not improve the outcome of DSS-induced colitis in IMQ mice. It is possible that *Lactobacillus* species were insufficient to ameliorate DSS colitis once gut B cells were reduced below a certain threshold. Antibiotic therapy in IMQ mice ameliorated colitis because this prevented the induction of pathogenic microbiome conditions in the gut during DSS administration. We also assessed whether psoriasis-like dermatitis worsened under conditions of colitis. However, we could not observe any differences in the dermatitis of DSS-treated mice compared with water-treated mice (data not shown). Dermatitis induced dysbiosis and exacerbated colitis, but the opposite did not occur in our model.

Potential correlations between IBD and psoriasis have been explored using clinical evidence, including the overlap of patients with the 2 diseases, gut microbe similarities among patients with these conditions, and the success of anti-TNF- $\alpha$  or anti-IL12/23p40 antibody therapies in human diseases. Further studies are needed to fill the gaps between human clinical disease and mouse experimental models. To this end, we showed that IMQ-induced psoriasis-like dermatitis reduced IgD<sup>+</sup> and IgM<sup>+</sup> B cells in the gut and altered the composition of the gut microbiome. We also showed that the dysbiosis in IMQ mice involved colitogenic microbes that exacerbated DSS colitis. Further studies are

**Figure 6. (See previous page). A gut microbiome in IMQ mice is essential to induce severe DSS colitis.** (A) Mice were administered a mixture of ampicillin, neomycin, vancomycin, and metronidazole by oral gavage 3 times a week until the end of the experiment. IMQ treatment was started 1 week after starting Abx treatment. Colonic lamina propria mononuclear cells after IMQ treatment (on day 17) were analyzed by flow cytometry. (B and C) Flow cytometry analysis, the ratio and cell number of CD11b<sup>+</sup>CD64<sup>+</sup> cells in CD45<sup>+</sup>CD3<sup>-</sup>CD19<sup>-</sup>B220<sup>-</sup>NK1.1<sup>-</sup> cells from colon lamina propria mononuclear cells. (D and E) Flow cytometry analysis, the ratio and cell number of CD19<sup>+</sup> cells in CD45<sup>+</sup> cells from colon lamina propria mononuclear cells. (F-H) Percentage in the total B cells (left) and absolute number (right) of (F) IgA<sup>+</sup> B cells, (G) IgD<sup>+</sup> B cells, and (H) IgM<sup>+</sup> B cells in CD45<sup>+</sup> cells from colon lamina propria mononuclear cells. (I) Mice were administered Abx (a mixture of ampicillin, neomycin, vancomycin, and metronidazole) or distilled water by oral gavage 3 times a week until the end of the experiment. Topical IMQ treatment was started 1 week after starting Abx or distilled water. A total of 2% (wt/vol) DSS subsequently was administered to all mice for 7 days after topical treatment of IMQ or vehicle. (J) Psoriasis Area and Severity Index (PASI) score on day 16 of IMQ or vehicle treatment. (K) Body weight changes during administration of DSS. (L) Body weight percentages on day 7 of DSS colitis. (M) Representative photograph of colon on day 7 of DSS colitis. (N) Colon length on day 7 of DSS colitis. (O) DAI score on day 7 of DSS colitis. (P) Representative H&E staining of distal colon section on day 7 of DSS colitis. Scale bar: 100  $\mu$ m. (Q) Histologic score for colitis on day 7 of DSS colitis (water-cont-DSS and water-IMQ-DSS, n = 11; Abx-cont-DSS, n = 9; Abx-IMQ-DSS, n = 7). Each symbol represents an individual mouse. Statistical analyses were performed with the Student *t* test or 1-way analysis of variance followed by the Tukey multiple comparison test. \**P* < .05, \*\**P* < .01, \*\*\**P* < .001. Error bars represent the SEM of samples within a group. Data are pooled from 2 independent experiments.





needed to investigate the precise mechanisms connecting dermatitis, intestinal immune cells, and the gut microbiome. Our findings shed novel light on the skin–gut interaction and potentially may lead to the development of new therapeutic targets for IBD patients with psoriasis.

## Materials and Methods

### Animals

C57BL/6J female mice and IQI/Jic (germ-free ICR) mice were purchased from Japan CLEA (Tokyo, Japan). TLR7<sup>-/-</sup> mice were purchased from Oriental Bio Service (Tokyo, Japan). Mice, except for the GF mice, were maintained under specific pathogen-free (SPF) conditions. GF mice were bred and maintained in vinyl isolators. All experiments were approved by the Institutional Review Board for Animal Experiments at Keio University and were performed according to the institutional guidelines and home office regulations.

### IMQ-Induced Psoriasis-Like Dermatitis

At 7–8 weeks of age, mice were shaved on the back skin under anesthesia. For anesthesia, a mixture of medetomidine (0.3 mg/kg, 002949, lot 705160; Domitor; Nippon Zenyaku Kogyo, Tokyo, Japan), midazolam (4.0 mg/kg, 27803229, lot FW3745; Sandoz, Holzkirchen, Germany), and butorphanol (5.0 mg/kg, 005526, lot VETLF5; Vetorphale; Meiji Seika Pharma, Tokyo, Japan) was injected IP. After shaving, commercially available 5% IMQ cream (02507936, lot GSJ115A, Beselna Cream; Mochida Pharmaceutical) was applied topically (62.5 mg) on the backs of the mice for 6 consecutive days, followed by 3 days for rest. After 1 cycle for 9 days, mice were again treated for another cycle (12 days of application of IMQ in total). Vehicle cream (286202303, lot 8H38; Vaseline; KENEI Pharmaceutical, Tokyo, Japan) was applied topically on the shaved back of mice from the control group according to the same schedule as the IMQ group. To assess the severity of psoriasis-like dermatitis, the clinical Psoriasis Area and Severity Index score was calculated. Erythema, scaling, and thickening

were scored independently on a scale from 0 to 4: 0, none; 1, slight; 2, moderate; 3, marked; and 4, very marked. Each score was added and the total scores were provided.

### DSS-Induced Colitis or Induction of Acute Experimental Colitis

C57BL/6J mice and IQI mice were administered 2% (wt/vol) and 3% (wt/vol) DSS (molecular weight, 36,000–50,000 daltons, 160110, lots M7191 and Q3526; MP Biomedicals, Santa Ana, CA), respectively, dissolved in sterile distilled water ad libitum for 7 days. SPF mice were weighed every day to determine the percentage of body weight loss from baseline. Body weight loss, stool consistency, and rectal bleeding were evaluated and scored for DAI. No weight loss was registered as 0, weight loss of 1% to 5% from baseline was assigned 1 point, weight loss of 6% to 10% from baseline was assigned 2 points, weight loss of 11% to 20% from baseline was assigned 3 points, and weight loss of more than 20% from baseline was assigned 4 points. For stool consistency, 0 points were assigned for well-formed pellets, 2 points for pasty and semiformal stools that did not adhere to the anus, and 4 points for liquid stools that adhered to the anus. For bleeding, 0 was assigned for no blood, 2 points for positive bleeding, and 4 points for gross bleeding.

### Histology

A distal colon section after DSS-induced colitis and a skin section after induction of psoriasis-like dermatitis were collected and fixed with 10% formalin (068-03841, lot TWE1483; Wako, Tokyo, Japan). The fixed samples were embedded in paraffin, and stained with H&E at Morphotechnology Co, Ltd (Sapporo, Japan). To evaluate the severity of DSS-induced colitis, histologic scores were determined with the colon section as previously described.<sup>20</sup> Briefly, 3 independent parameters—extent, inflammation, and crypt damage—were assessed and scored as follows: extent: scored 0 to 3 (0, none; 1, mucosa; 2, submucosa; 3, transmural); inflammation: scored 0 to 3 (0, none; 1, slight;

**Figure 7. (See previous page). Fecal microbiome transplantation of IMQ mice exacerbated DSS colitis.** (A) GF mice were transplanted with a fecal microbiome derived from control mice (cont gnoto mice) or IMQ-treated mice (IMQ gnoto mice). Three weeks after transplantation, immune cells were analyzed by flow cytometry. (B) Percentage (*left*) and absolute number (*right*) of CD11b<sup>+</sup>CD64<sup>+</sup> cells in CD45<sup>+</sup>CD3<sup>+</sup>CD19<sup>-</sup>B220<sup>-</sup>NK1.1<sup>-</sup> cells from colonic lamina propria. (C) Percentage (*left*) and absolute number (*right*) of B cells in CD45<sup>+</sup> colonic lamina propria. (D) Percentage of IgA<sup>+</sup> (*left*), IgD<sup>+</sup> (*middle*), and IgM<sup>+</sup> (*right*) B cells in the total B cells from colonic lamina propria (n = 6–7 in each group). (E) Experimental protocol. Cont gnoto mice and IMQ gnoto mice (shown in panel A) were further induced with acute colitis by 3% (wt/vol) DSS. After administration of DSS for 7 days, the severity of colitis was assessed. (F) Representative photograph of colon on day 7 of DSS colitis. (G) Body weight on day 7 of DSS colitis. (H) Colon length on day 7 of DSS colitis. (I) Partial DAI score on day 7 of DSS colitis. Partial DAI score was calculated as the sum of scores for perianal bleeding (0–4) and diarrhea (0–4) (part of the DAI score except for the body weight loss component). (J) Representative H&E staining of distal colon section on day 7 of DSS colitis. Scale bar: 100 μm. (K) Histologic score of colitis on day 7 of DSS (n = 3–5 in each group). (L) Experimental protocol. Mice treated with IMQ or vehicle subsequently were induced with colitis by 2% (wt/vol) DSS for 7 days. Feces derived from control mice, or saline, was administered daily by oral gavage, from the day before starting DSS to the end of the experiment. (M) Body weight changes during administration of DSS and (N) the percentage of the initial value (day 0 of DSS) of body weight on day 7 of DSS colitis. (O) DAI score on day 7 of DSS colitis (n = 6 in each group). (P) Experimental protocol. Mice treated with IMQ or vehicle were subsequently induced with colitis by 2% (wt/vol) DSS for 7 days. A mixture of *L. johnsonii* and *L. reuteri*, or saline, was administered daily by oral gavage, from the day before starting DSS to the end of the experiment. (Q) Body weight changes during administration of DSS and (R) the percentage of the initial value (day 0 of DSS) of body weight on day 7 of DSS colitis. (S) DAI score on day 7 of DSS colitis (n = 8 in each group). Each symbol represents an individual mouse. Statistical analyses were performed with the Student *t* test. \**P* < .05, \*\**P* < .01, \*\*\**P* < .001. Error bars represent the SEM of samples within a group.

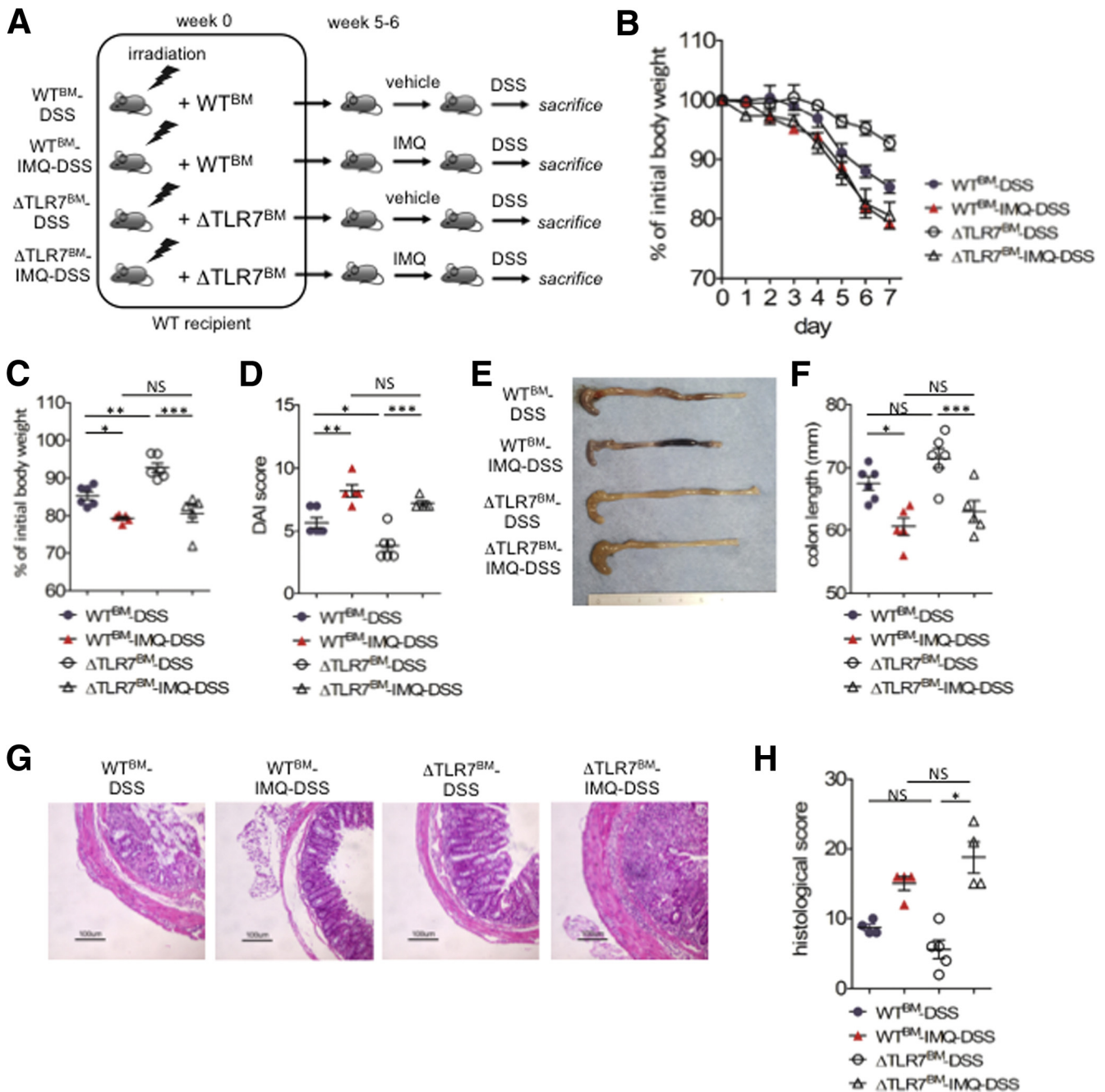


**Figure 8. Both hematopoietic and nonhematopoietic TLR7-positive cells enhance IMQ-DSS colitis.** (A) Experimental protocol. (B) Body weight changes during administration of DSS. (C) Body weight on day 7 of DSS colitis. (D) DAI score on day 7 of DSS colitis. (E) Representative photograph of colon on day 7 of DSS colitis. (F) Colon length on day 7 of DSS colitis. (G) Representative H&E staining of distal colon section on day 7 of DSS colitis. Scale bar: 100  $\mu$ m. (H) Histologic score for colitis on day 7 of DSS colitis. Each symbol represents an individual mouse (n = 5–6). Statistical analyses were performed with 1-way analysis of variance followed by the Tukey multiple comparison test. \* $P < .05$ , \*\* $P < .01$ , \*\*\* $P < .001$ . Error bars represent the SEM of samples within a group.

2, moderate; 3, severe); crypt damage: scored 0 to 4 (0, none; 1, basal one-third lost; 2, basal two-thirds lost; 3, only surface epithelium intact; 4, entire crypt and epithelium lost) were multiplied by scores of spreads that were from 1 to 4 (1, 0%–25%; 2, 26%–50%; 3, 51%–75%; 4, 76%–100%). Each multiplied score was summed and defined as a histologic score (0–40).

#### Preparation of Colonic Lamina Propria Mononuclear Cells and Colonic Epithelial Cells

A mouse was euthanized by cervical dislocation and the colon was collected without mesentery. The colon was opened longitudinally and washed with  $\text{Ca}^{2+}$ ,  $\text{Mg}^{2+}$ -free Hank's balanced salt solution (HBSS) (17460-15, lot

L8A4406; Nacalai Tesque, Tokyo, Japan) to remove fecal content. After washing, the colon was further cut into small pieces and incubated with HBSS containing 1 mmol/L dithiothreitol (15508-013; lot H1095A0517; Invitrogen, Carlsbad, CA) and 5 mmol/L EDTA (15575038; lot 1624957; Thermo Fisher Scientific, Waltham, MA) for 30 minutes at 37°C to remove the epithelial layer. After removal of the epithelial layer, the mucosal pieces were washed with HBSS and dissolved in solution by incubation with HBSS containing 1.5% fetal bovine serum (10270-106, lot 42Q1074K; Thermo Fisher Scientific), 1.0 to 3.0 mg/mL collagenase (032-22364, lot PTQ3925; Wako), and 0.1 mg/mL DNase (DN25-1G, lot SLBV1446; Sigma-Aldrich, St. Louis, MO) for 1 hour at 37°C. The dissolved solution was centrifuged at 1700 rpm for 5 minutes, and the pellet was resuspended in 40% Percoll (17-0891-01, lot 10262818; GE Healthcare, Chicago, IL) and overlaid on 75% Percoll. Percoll gradient separation was performed by centrifugation at 2000 rpm for 20 minutes at 20°C. Lamina propria mononuclear cells were collected at the interphase between 40% and 75% Percoll layers. For colonic epithelial cells, the supernatant containing the removed epithelial layer as described earlier was collected and centrifuged at 1700 rpm for 5 minutes at 4°C and the pellet was resuspended in 40% Percoll. Percoll gradient separation was performed as well. Epithelial cells, existing in the upper layer, were collected, washed, and resuspended with appropriate buffer. Colonic lamina propria CD11b<sup>+</sup> cells (LP CD11b<sup>+</sup>s) were obtained from colonic lamina propria mononuclear cells by positive selection with anti-CD11b MACS beads (130-049-601, lot 5151216079; Miltenyi Biotech, Cologne, Germany), according to the manufacturer's instructions.

### *Preparation of Epidermal and Dermal Cell Suspensions*

Back skin was harvested from mice after shaving. The skin tissue was floated with the epidermal side up in 5 mL of trypsin-EDTA solution and 0.05% trypsin-0.53 mmol/L EDTA × 4 Na (32778-34, lot L7R3660; Nacalai Tesque) and incubated at 37°C for 30 minutes. The epidermis and dermis were separated with forceps. The epidermal tissue was loosened by suction with a 50-mL syringe repeatedly and cells were passed through a cell strainer (352360, lot 147164; Corning, New York, NY) and collected. Dermis was cut into small pieces using scissors, and then incubated in 4 mL of RPMI-1640 containing 0.03% (wt/vol) Liberase TL grade (05401020001, lot 29195900; Roche) and 10 U/mL of DNase I (10104159001, lot 12487400; Roche, Basel, Switzerland) for 60 minutes at 37°C, shaking with rotation at 200 rpm, and the lysate was passed through a cell strainer and the filtered dermal cells were collected.

### *Preparation of Skin Draining Lymph Node and Mesenteric Lymph Node Cell Suspensions*

Skin draining lymph nodes, proper axillary lymph nodes, and subiliac lymph nodes were harvested from mice after death. Mesenteric lymph nodes also were harvested as well.

Fat tissues around these lymph nodes were removed carefully and the lymph nodes were homogenized manually in HBSS and the lysates were filtered through a cell strainer, and the passed cells were collected for analysis.

### *Preparation of Spleen Cell Suspensions*

Spleen was harvested from mice after death and homogenized manually in HBSS. The lysates were filtered through a cell strainer. The passed cells were hemolyzed with 0.84% (vol/wt) ammonium chloride (02424-55, lot M8E1936; Nacalai), washed with HBSS, and collected for analysis.

### *Isolation of Peritoneal Cells*

Mice were euthanized with isoflurane (099-06571; Wako) and injected with 5 mL of cold PBS IP. After injection, the abdomen was gently massaged and the injected fluid was collected as much as possible.

### *Flow Cytometry*

The surface antigens of isolated single-cell suspensions were pre-incubated with an FcγR-blocking monoclonal antibody (anti-mouse CD16/32, 2.4G2, 553142, lot 7248907; BD Biosciences, San Diego, CA) for 20 minutes before staining cell surface antigens. After FcγR blocking, fluorescence-conjugated specific monoclonal antibodies to surface molecules were incubated at 4°C and protected from light for 30 minutes. After staining surface molecules, the cells were washed and resuspended with PBS containing 0.5% (wt/vol) bovine serum albumin (BSA) (01863-48, lot M7G7120; Nacalai). For flow cytometry analysis, the FACS Canto II system (BD Biosciences), which is available for 8 colors, was used. Data were analyzed by FlowJo Vx software (Tree Star). The monoclonal antibodies used for staining included the following: FITC anti-IgA (10-3, 559354, lot 5089919), FITC anti-CD4 (RM4-5, 553047, lot 4247833), phycoerythrin (PE) anti-CD64 (X54-5/7.1.1, 558455, lot 2125512), PE anti-CD19 (1D3, 553786, lot 37168), PerCP-Cy5.5 7-amino-actinomycin D (7-AAD, 5168981E, lot 5006667-1), PerCP-Cy5.5 anti-CD4 (RM4-5, 56115, lot 7027622/602570), PE-Cy7 anti-CD3 (145-2C11, 552774, lot 6251919), APC-Cy7 anti-CD3 (145-2C11, 557596, lot 5163789), APC-Cy7 anti-CD19 (1D3, 557655, lot 5168575), APC-Cy7 anti-B220 (RA3-6B2, 552094, lot 7090802), APC anti-CD138 (281-2, 142506, lot 8197973), and Brilliant Violet 510 anti-CD45 (30-F11, 563891, lot 7293934) were purchased from BD Biosciences. FITC anti-CD11b (M1/70, 11-0112-82, lot 4283564), FITC anti-IFN-γ (XMG1.2, 11-7311-82, lot 4332573), PE anti-IL17A (eBio17B7, 12-7177-81, lot 4306419), and APC anti-Foxp3 (FJK-16s, 17-5773-80, lot E07302-1636) were purchased from eBioscience. PE anti-IgM (RMM-1, 406508, lot B106128), PE-Cy7 anti-B220 (RA3-6B2, 103222, lot B139371), PE-Cy7 anti-CD80 (16-10A1, 104734, lot B181277), APC anti-CD206 (C068C2, 141707, lot B218213), APC-Cy7 anti-NK1.1 (PK136, 108724, lot B225146), Brilliant Violet 421 anti-IgD (11-26c.2a, 405725, lot B244155), and Brilliant Violet 121 anti-CD3 (145-2C11, 100341, lot B220025) were purchased from BioLegend (San Diego, CA).



### Intracellular Staining for Flow Cytometry

For intracellular cytokine staining, cells were incubated for 4 hours in a humidified incubator with 5% CO<sub>2</sub>, in RPMI-1640 medium containing 10% fetal bovine serum and 1% penicillin/streptomycin (15140-122, lot 1622132; Thermo Fisher Scientific) with 50 ng/mL phorbol 12-myristate-13-acetate (PMA) (P1585-1MG, lot SLBN5870V; Sigma-Aldrich), 500 ng/mL ionomycin (10634-1MG, lot 127M4002V; Sigma-Aldrich), 50 ng/mL recombinant mouse IL23 (14-8231-63, lot 4299410; eBioscience), and GolgiStop (51-2092KZ, lot 6308707; BD Bioscience). After incubation, FcγR blocking and surface antigen staining were performed as described earlier. After that, dead cells were stained with Fixable Viability Dye eFluor 780 (65-0865-14, lot 4333604; eBioscience) for 30 minutes at 4°C and protected from light. The cells were washed and incubated with fixation/permeabilization solution (00-5123-43, lot 1954346 and 00-5223-56, lot 4333317; Invitrogen) overnight at 4°C protected from light. Then intracellular cytokine was stained by fluorescence-conjugated monoclonal antibodies incubated for 30 minutes at 4°C and protected from light. The incubated cells were washed and analyzed by flow cytometry. For staining of Foxp3-positive cells, the same procedure but without stimulation with PMA, ionomycin, and IL23, was performed.

### Quantitative Real-Time Polymerase Chain Reaction

Total RNA was extracted from single-cell suspensions by the RNeasy Mini Kit (74106, lot 157045393; Qiagen, Venlo, Netherlands) or the RNeasy Micro Kit (74004, lot 154052961; Qiagen) according to the manufacturer's instructions. The complementary DNA was synthesized from the extracted RNA via reverse-transcription using the iScript complementary DNA Synthesis Kit (170-8891, lot 64086966; Bio-Rad, Hercules, CA) according to the manufacturer's instructions. The obtained complementary DNA was amplified by quantitative real-time polymerase chain reaction (PCR) using primer sets (Table 1) and the SYBR Green FAST qPCR Master Mix kit (KK4602, lot 004569-4-1; Kapa Biosystems, Wilmington, MA), and gene expression was quantified by comparative cycle threshold method. *Rpl32* was used as the internal control and relative gene expression was determined compared with the expression of internal control. For PCR reactions, samples were heated at 95°C for 3 minutes at first, and repeated for 40 cycles of the following 2 steps: 95°C for 3 seconds and 60°C for 20 seconds. The quantitative real-time PCR was performed by the Step OnePlus real-time PCR system (Thermo Fisher Scientific).

### Cytokine Assay of Colonic Lamina Propria CD11b<sup>+</sup> Cells

LP CD11b<sup>+</sup>s were seeded on 96-well tissue culture plates (5 × 10<sup>5</sup> cells/mL, 1 × 10<sup>5</sup>/well) in RPMI-1640 medium containing 10% fetal bovine serum and 1% penicillin/streptomycin (15140-122, lot 1622132; Thermo Fisher Scientific), and stimulated with lipopolysaccharide

**Table 1.** Quantitative Real-Time PCR Primer Sequences

Primer list 5'-3'
Rpl32 forward: ACAATGTCAAGGAGCTGGAG
Rpl32 reverse: TTGGGATTGGTGACTCTGATG
IL6 forward: ACCAGAGGAAATTTCAATAGGC
IL6 reverse: TGATGCACTGCAGAAAACA
IL10 forward: CCCATTCTCGTCACGATCTC
IL10 reverse: TCAGACTGGTTTGGGATAGGTTT
IL12β forward: TGGTTTGCCATCGTTTTGCTG
IL12β reverse: ACAGGTGAGGTTCACTGTTTCT
Tnf-α forward: AGGGTCTGGGCCATAGAAGT
Tnf-α reverse: CCACCACGCTCTTCTGTCTAC
Arg1 forward: CTCCAAGCCAAAGTCTTAGAG
Arg1 reverse: AGGAGCTGTCATTAGGGACATC
Nos2 forward: GTTCTCAGCCCAACAATAACAAGA
Nos2 reverse: GTGGACGGGTGCGATGTCAC
ZO-1 forward: TGTCAGGCATTGGCTAGAGGTTT
ZO-1 reverse: GGCCAAGGCCATAATAAACTTTGAG
Occludin forward: GAGTTAACGTCGTGGACCGGTATC
Occludin reverse: CCCTGAAATACAAAGGCAGGAATG
RegIIIγ forward: TTCCTGTCTCCATGATCAAAA
RegIIIγ reverse: CATCCACCTCTGTTGGGTTCA

Sequences of each primers used in the experiments are shown.

(100 ng/mL) (L3012, lot 123M4094V; Sigma) or peptidoglycan (10 μg/mL) (tlrl-pgnsa, lot PSA-36-01; Invitrogen) for 24 hours at 37°C in a humidified incubator with 5% CO<sub>2</sub>. After incubation, the culture supernatants were collected and stored at -80°C until analysis. For measurement of secreted cytokines in the culture supernatants, a cytometric bead array Mouse Inflammation Kit (552364, 5261593; BD Biosciences) was used and analyzed with a FACS Canto II flow cytometer (BD Biosciences).

### Western Blot Analysis

Proteins were extracted using the M-PER Mammalian Protein Extraction Reagent (78501, lot PL209289; Thermo Fisher Scientific). The protein was denatured with 2-mercaptoethanol (1610710, lot 1071172; Bio-Rad) and sodium dodecyl sulfate by boiling at 99°C for 5 minutes, and polyacrylamide gel electrophoresis was performed with Mini-Protean TGX Gels (456-1096, lot 64121225; Bio-Rad) and Tris/glycine/sodium dodecyl sulfate buffer (1610772, lot 64087453; Bio-Rad) (sodium dodecyl sulfate-polyacrylamide gel electrophoresis). After sodium dodecyl sulfate-polyacrylamide gel electrophoresis, blotting to polyvinylidene difluoride membrane was performed at 60 V for 2 hours in Tris/glycine buffer (1610771, lot 64082418; Bio-Rad). After blotting, polyvinylidene difluoride membrane was rinsed and blocking was performed with 4% (vol/wt) skim milk (190-12865, lot LKR1611; Wako) for 1 hour at room temperature. Antibodies against β-actin (4967S, lot 6; Cell Signaling Technology, Tokyo, Japan),

NLRP3 (AG-20B-0014-C100, lot A27381510; AdipoGen, San Diego, CA), and occludin (ab216327, lot GR3193464-11; Abcam, Cambridge, UK) were used. Signal detection was performed using Clarity Western ECL Substrate (1705061, lot 102030523; Bio-Rad) and ImageQuant LAS 4000 (GE Healthcare). Densitometric analysis was performed using ImageQuant TL (GE Healthcare).

### 16S rRNA Metagenomic Analysis

The extraction of bacterial DNA was obtained from the samples of fecal content. The hypervariable V3–V4 region of the 16S gene was amplified using Ex Taq Hot Start (RR006A, lot AI20308A; Takara, Tokyo, Japan) and subsequently purified using AMPure XP (A63881, lot 15023200; Beckman Coulter, Atlanta, GA). Mixed samples were prepared by pooling approximately equal amounts of each amplified DNA and sequenced using the Miseq Reagent Kit V3 (600 cycle, 15043895, lot 10046122; Illumina, San Diego, CA) and the Miseq sequencer (Illumina), according to the manufacturer's instructions. Sequences were analyzed using the QIIME software package version 1.9.1.<sup>36,37</sup> Paired-end sequences were joined using a fastq-join tool in the ea-utils software package.<sup>38</sup> High-quality sequences per sample (15,000) were chosen randomly from the quality filter-passed sequences. After trimming off both primer sequences using cutadapt<sup>39</sup> following chimera detection by USEARCH<sup>40</sup> de novo method, the sequences were assigned to OTUs using the UCLUST algorithm<sup>41</sup> with a sequence identity threshold of 96%. Taxonomic assignments of each OTU were made by similarity searching against the publicly available 16S (RDP version 10.27 and CORE update September 2, 2012) and the NCBI genome database using the GLSEARCH program.

### Antibiotic Treatment

To eliminate as much bacteria in the gut of SPF mice as possible, 4 antibiotics—ampicillin (6.7 mg/mL, A9518-25G, lot BCBR6229V; Sigma-Aldrich), neomycin (6.7 mg/mL, N1876-25G, lot SLBN9098V; Sigma-Aldrich), vancomycin (3.35 mg/mL, 226-01306, lot LKF6780; Wako), and metronidazole (6.7 mg/mL, M3761-25G, lot MKBZ3056V; Sigma-Aldrich)—were mixed and dissolved in sterile distilled water in the final concentrations described earlier to target gram-positive and gram-negative bacteria broadly, and were administered to mice (500  $\mu$ L per mouse) by oral gavage 3 times a week.<sup>31</sup> The same amount of sterile distilled water was given to mice in the control group on the same schedule. In the experiments using antibiotics, they were given to the mice until death.

### Fecal Microbiome Transplantation

Feces were derived from IMQ-treated and untreated C57BL/6J mice and stored at  $-80^{\circ}\text{C}$  until use. The feces were dissolved in 1.5 mL PBS homogenized, and then filtered through a 100- $\mu\text{m}$  nylon mesh strainer (352360, lot 147164; Corning). The filtered contents were resuspended with PBS in a total volume of 2 mL, of which 150  $\mu$ L per mouse was administered to GF mice in the vinyl isolator, or

5 mL, of which 300  $\mu$ L per mouse was administered to SPF mice by oral gavage.

### Oral Administration of *Lactobacillus* Species

A single strain of *L johnsonii* was isolated by cultivation with fecal samples derived from C57BL/6J wild-type SPF mice. Feces were cultured on MRS selective agar (288210, lot 5272510; BD Biosciences) at  $37^{\circ}\text{C}$  for 48 hours anaerobically. The single colonies were collected and screened by PCR with the specific primer for *L johnsonii* (5'-CACTA GACGCATGTCTAGAG-3' and 5'-AGTCTCTCAACTCGGCTATG-3'),<sup>32</sup> and then identified by full-length 16S rRNA gene sequencing (Techno Suruga Lab, Shizuoka, Japan). A single strain of *L reuteri* was purchased from American Type Culture Collection (ATCC23272). The isolated single strain of *L johnsonii* and a single strain of *L reuteri* were cultured on MRS selective broth (288130, lot 4307971; BD Biosciences) for 24 hours anaerobically and centrifuged at 1700 rpm for 5 minutes. The deposit was dissolved in sterile saline and then administered to SPF mice once a day by oral gavage.

### Bone Marrow Transplantation

Bone marrow was isolated from WT and TLR7<sup>-/-</sup> mice. Bone marrow was obtained by flushing the femurs and tibiae of donor mice with RPMI-1640 (30264-85, lot L8H5874; Nacalai Tesque). Recipient WT mice were lethally irradiated with 11 Gy whole-body  $\gamma$  irradiation (MBR-1520R-3; Hitachi Co Ltd, Hitachi, Japan). After irradiation, the recipient mice then were injected intravenously with  $5 \times 10^6$  bone marrow cells via tail vein. Mice then were housed for 6 weeks to allow full engraftment of the bone marrow.

### Immunofluorescence

Paraffin-embedded distal colon sections from mice after induction of psoriasis-like dermatitis were used for analysis by immunofluorescence. Antigen retrieval was performed in boiled citric acid solution followed by blocking procedure. The sections were blocked with Block Ace (UKB80, lot STK102796; DS Pharma Biomedical Co, Ltd, Tokyo, Japan) for 60 minutes at room temperature. After blocking, the sections were incubated with primary antibodies overnight at  $4^{\circ}\text{C}$ . The primary antibodies were diluted with Dako Antibody Diluent (S3022, lot 10125945; Dako) at the following dilution rates. Mouse anti-occludin antibody (33-1500, lot SB231108; Abcam) and rabbit anti-ZO-1 polyclonal antibody (61-7300, lot SH252320; Invitrogen) were both at 1:100, and rabbit anti-claudin 2 antibody (ab53032, lot GR314368-12; Abcam) was at 1:200. After rinsing, the sections were incubated with fluorescence-conjugated secondary antibodies as follows, for 2 hours at room temperature while protected from light. Alexa Fluor 647-conjugated donkey anti-mouse IgG (ab150107, lot GR292574-3; Abcam), Alexa Fluor 488-conjugated donkey anti-rabbit IgG (ab150073, lot GR3191541; Abcam) both were diluted at 1:250. After rinsing, the sections were mounted with mounting medium and visualized by using an LSM 710 confocal laser scanning microscope (Carl Zeiss,

Oberkochen, Germany) equipped with ZEN, a modular image-processing and analysis software package for digital microscopy. Quantitative analysis for immunofluorescence images were performed by using ImageJ software (National Institutes of Health, Bethesda, MD).

### *Intraperitoneal Injection of IMQ*

For systemic administration of IMQ, imiquimod (R837) (tlrl-imq, lot IMQ-36-02A; Invivogen) was dissolved with endotoxin-free water at 1 mg/mL and injected IP (10 mg/kg) daily for a week.

### *Enzyme-Linked Immunosorbent Assay for Measurement of Fecal IgA*

Feces derived from mice were dissolved in PBS containing 1% (wt/vol) BSA and 0.05% (vol/vol) Tween20 at a concentration of 100 mg/mL, and homogenized. To remove debris, these homogenized samples were centrifuged stepwise with increasing force (400×g for 5 min, 8000×g for 10 min, and 19,000×g for 10 min). The supernatant was collected and the IgA concentration was measured by IgA Mouse Enzyme-Linked Immunosorbent Assay kit (88-50450-88, lot 146856016; Thermo Fisher Scientific) according to the manufacturer's instructions. The absorbance was measured at a wavelength of 450 nm and the reference wave length was 550 nm using Infinite F200 PRO (Tecan, Männedorf, Switzerland).

### *Analysis for Fecal IgA-Coated Bacteria*

Feces were collected and dissolved in PBS, homogenized, and filtered through a 40- $\mu$ m nylon mesh strainer. The filtered contents were centrifuged at 9000×g for 10 minutes at 4°C and the supernatant was discharged. The deposits were resuspended with 10 mL PBS and centrifuged twice as well. The deposit then was resuspended with PBS in a total volume of 2 mL and then centrifuged at 50×g for 5 minutes at 4°C, and the supernatant was collected. The collected supernatant was first stained for bacteria with the Bacteria Counting Kit for flow cytometry (B7277, lot 1868123; Thermo Fisher Scientific) according to the manufacturer's instructions. Then the samples were washed with PBS, and incubated with 1% (wt/vol) BSA/PBS containing rat serum (R9759-5ML, lot SLBR6771V; Sigma-Aldrich) for blocking on ice for 30 minutes. The incubated samples subsequently were stained by PE anti-IgA (12-4204-83, lot E01650-1634; eBioscience) or PE Rat-IgG1 $\kappa$  isotype control (12-4301-82, lot E01654-1633; eBioscience) for 30 minutes on ice and protected from light. The samples were washed with 1% BSA/PBS and centrifuged twice and analyzed by flow cytometry.

### *Analysis for Intestinal Permeability With FITC-Dextran*

Intestinal permeability was assessed by administration of FITC-dextran (average molecular weight, 4 kilodaltons and 70 kilodaltons, respectively, FD4-250MG, lot

BCBS4210V and FD70S-100MG, lot SLBT8689; Sigma-Aldrich) with slight modification. Briefly, mice were kept fasting for 6 hours before administration of FITC-dextran. A total of 60 mg/kg FITC-dextran was given to mice by oral gavage or IP injection, and the plasma concentration of FITC-dextran was determined by fluorescence intensity at 1, 2, and 4 hours after administration of FITC-dextran. The fluorescence intensity was measured by Infinite F200 PRO (Tecan).

### *Statistical Analysis*

The results are expressed as means  $\pm$  SEM. Groups of data were compared with 1-way analysis of variance with the Tukey multiple comparison post hoc analysis or the Student *t* test or Mann-Whitney *U* test, except for the principal coordinate analysis for the gut microbiome. The differences in the principal coordinate analysis were analyzed with the Permanova test. The difference was considered significant when the *P* value was less than .05.

### **References**

1. Parisi R, Symmons DP, Griffiths CE, Ashcroft DM, Identification and Management of Psoriasis and Associated Comorbidity (IMPACT) Project Team. Global epidemiology of psoriasis: a systematic review of incidence and prevalence. *J Invest Dermatol* 2013;133:377–385.
2. Drago L, De Grandi R, Altomare G, Pigatto P, Rossi O, Toscano M. Skin microbiota of first cousins affected by psoriasis and atopic dermatitis. *Clin Mol Allergy* 2016; 14:2.
3. Zakostelska Z, Malkova J, Klimesova K, Rossmann P, Hornova M, Novosadova I, Stehlikova Z, Kostovcik M, Hudcovic T, Stepankova R, Juzlova K, Hercogova J, Tlaskalova-Hogenova H, Kverka M. Intestinal microbiota promotes psoriasis-like skin inflammation by enhancing Th17 response. *PLoS One* 2016;11:e0159539.
4. Protic M, Schoepfer A, Yawalkar N, Vavricka S, Seibold F. Development of psoriasis in IBD patients under TNF-antagonist therapy is associated neither with anti-TNF-antagonist antibodies nor trough levels. *Scand J Gastroenterol* 2016;51:1482–1488.
5. Cargill M, Schrodi SJ, Chang M, Garcia VE, Brandon R, Callis KP, Matsunami N, Ardlie KG, Civello D, Catanese JJ, Leong DU, Panko JM, McAllister LB, Hansen CB, Papenfuss J, Prescott SM, White TJ, Leppert MF, Krueger GG, Begovich AB. A large-scale genetic association study confirms IL12B and leads to the identification of IL23R as psoriasis-risk genes. *Am J Hum Genet* 2007;80:273–290.
6. Liu Y, Helms C, Liao W, Zaba LC, Duan S, Gardner J, Wise C, Miner A, Malloy MJ, Pullinger CR, Kane JP, Saccone S, Worthington J, Bruce I, Kwok PY, Menter A, Krueger J, Barton A, Saccone NL, Bowcock AM. A genome-wide association study of psoriasis and psoriatic arthritis identifies new disease loci. *PLoS Genet* 2008;4:e1000041.
7. Eppinga H, Poortinga S, Thio HB, Nijsten TEC, Nuij V, van der Woude CJ, Vodegel RM, Fuhler GM,



- Peppelenbosch MP. Prevalence and phenotype of concurrent psoriasis and inflammatory bowel disease. *Inflamm Bowel Dis* 2017;23:1783–1789.
8. Wu JJ, Nguyen TU, Poon KY, Herrinton LJ. The association of psoriasis with autoimmune diseases. *J Am Acad Dermatol* 2012;67:924–930.
  9. Lee FI, Bellary SV, Francis C. Increased occurrence of psoriasis in patients with Crohn's disease and their relatives. *Am J Gastroenterol* 1990;85:962–963.
  10. Eppinga H, Sperna Weiland CJ, Thio HB, van der Woude CJ, Nijsten TE, Peppelenbosch MP, Konstantinov SR. Similar depletion of protective *Faecalibacterium prausnitzii* in psoriasis and inflammatory bowel disease, but not in hidradenitis suppurativa. *J Crohns Colitis* 2016;10:1067–1075.
  11. Scherl JU, Ubeda C, Artacho A, Attur M, Isaac S, Reddy SM, Marmon S, Neimann A, Brusca S, Patel T, Manasson J, Pamer EG, Littman DR, Abramson SB. Decreased bacterial diversity characterizes the altered gut microbiota in patients with psoriatic arthritis, resembling dysbiosis in inflammatory bowel disease. *Arthritis Rheum* 2015;67:128–139.
  12. Yang JY, Kim MS, Kim E, Cheon JH, Lee YS, Kim Y, Lee SH, Seo SU, Shin SH, Choi SS, Kim B, Chang SY, Ko HJ, Bae JW, Kweon MN. Enteric viruses ameliorate gut inflammation via Toll-like receptor 3 and Toll-like receptor 7-mediated interferon-beta production. *Immunity* 2016;44:889–900.
  13. Abt MC, Buffie CG, Susac B, Becattini S, Carter RA, Leiner I, Keith JW, Artis D, Osborne LC, Pamer EG. TLR-7 activation enhances IL-22-mediated colonization resistance against vancomycin-resistant enterococcus. *Sci Transl Med* 2016;8:327ra325.
  14. van der Fits L, Mourits S, Voerman JS, Kant M, Boon L, Laman JD, Cornelissen F, Mus AM, Florencia E, Prens EP, Lubberts E. Imiquimod-induced psoriasis-like skin inflammation in mice is mediated via the IL-23/IL-17 axis. *J Immunol* 2009;182:5836–5845.
  15. Terhorst D, Chelbi R, Wohn C, Malosse C, Tamoutounour S, Jorquera A, Bajenoff M, Dalod M, Malissen B, Henri S. Dynamics and transcriptomics of skin dendritic cells and macrophages in an imiquimod-induced, biphasic mouse model of psoriasis. *J Immunol* 2015;195:4953–4961.
  16. Van Belle AB, de Heusch M, Lemaire MM, Hendrickx E, Warnier G, Dunussi-Joannopoulos K, Fouser LA, Renaud JC, Dumoutier L. IL-22 is required for imiquimod-induced psoriasiform skin inflammation in mice. *J Immunol* 2012;188:462–469.
  17. Kanneganti TD, Body-Malapel M, Amer A, Park JH, Whitfield J, Franchi L, Taraporewala ZF, Miller D, Patton JT, Inohara N, Nunez G. Critical role for Cryopyrin/Nalp3 in activation of caspase-1 in response to viral infection and double-stranded RNA. *J Biol Chem* 2006;281:36560–36568.
  18. Viladomiu M, Kivolowitz C, Abdulhamid A, Dogan B, Victorio D, Castellanos JG, Woo V, Teng F, Tran NL, Sczesnak A, Chai C, Kim M, Diehl GE, Ajami NJ, Petrosino JF, Zhou XK, Schwartzman S, Mandl LA, Abramowitz M, Jacob V, Bosworth B, Steinlauf A, Scherl EJ, Wu HJ, Simpson KW, Longman RS. IgA-coated *E. coli* enriched in Crohn's disease spondyloarthritis promote TH17-dependent inflammation. *Sci Transl Med* 2017;9.
  19. Lee IA, Kim DH. *Klebsiella pneumoniae* increases the risk of inflammation and colitis in a murine model of intestinal bowel disease. *Scand J Gastroenterol* 2011;46:684–693.
  20. Jang SE, Lim SM, Jeong JJ, Jang HM, Lee HJ, Han MJ, Kim DH. Gastrointestinal inflammation by gut microbiota disturbance induces memory impairment in mice. *Mucosal Immunol* 2018;11:369–379.
  21. Liu HY, Roos S, Jonsson H, Ahl D, Dicksved J, Lindberg JE, Lundh T. Effects of *Lactobacillus johnsonii* and *Lactobacillus reuteri* on gut barrier function and heat shock proteins in intestinal porcine epithelial cells. *Physiol Rep* 2015;3.
  22. Ahl D, Liu H, Schreiber O, Roos S, Phillipson M, Holm L. *Lactobacillus reuteri* increases mucus thickness and ameliorates dextran sulphate sodium-induced colitis in mice. *Acta Physiol (Oxf)* 2016;217:300–310.
  23. Gao C, Major A, Rendon D, Lugo M, Jackson V, Shi Z, Mori-Akiyama Y, Versalovic J. Histamine H2 receptor-mediated suppression of intestinal inflammation by probiotic *Lactobacillus reuteri*. *MBio* 2015;6:e01358–e01315.
  24. Thomas CM, Saulnier DM, Spinler JK, Hemarajata P, Gao C, Jones SE, Grimm A, Balderas MA, Burstein MD, Morra C, Roeth D, Kalkum M, Versalovic J. Folate-mediated folate metabolism contributes to suppression of inflammation by probiotic *Lactobacillus reuteri*. *Microbiologyopen* 2016;5:802–818.
  25. Mackos AR, Galley JD, Eubank TD, Easterling RS, Parry NM, Fox JG, Lyte M, Bailey MT. Social stress-enhanced severity of *Citrobacter rodentium*-induced colitis is CCL2-dependent and attenuated by probiotic *Lactobacillus reuteri*. *Mucosal Immunol* 2016;9:515–526.
  26. Oliva S, Di Nardo G, Ferrari F, Mallardo S, Rossi P, Patrizi G, Cucchiara S, Stronati L. Randomised clinical trial: the effectiveness of *Lactobacillus reuteri* ATCC 55730 rectal enema in children with active distal ulcerative colitis. *Aliment Pharmacol Ther* 2012;35:327–334.
  27. Kirkland D, Benson A, Mirpuri J, Pifer R, Hou B, DeFranco AL, Yarovinsky F. B cell-intrinsic MyD88 signaling prevents the lethal dissemination of commensal bacteria during colonic damage. *Immunity* 2012;36:228–238.
  28. Riol-Blanco L, Ordovas-Montanes J, Perro M, Naval E, Thiriot A, Alvarez D, Paust S, Wood JN, von Andrian UH. Nociceptive sensory neurons drive interleukin-23-mediated psoriasiform skin inflammation. *Nature* 2014;510:157–161.
  29. Liu T, Xu ZZ, Park CK, Berta T, Ji RR. Toll-like receptor 7 mediates pruritus. *Nat Neurosci* 2010;13:1460–1462.
  30. Diogenes A, Ferraz CC, Akopian AN, Henry MA, Hargreaves KM. LPS sensitizes TRPV1 via activation of TLR4 in trigeminal sensory neurons. *J Dental Res* 2011;90:759–764.

31. Park CK, Xu ZZ, Berta T, Han Q, Chen G, Liu XJ, Ji RR. Extracellular microRNAs activate nociceptor neurons to elicit pain via TLR7 and TRPA1. *Neuron* 2014; 82:47–54.
32. Meseguer V, Alpizar YA, Luis E, Tajada S, Denlinger B, Fajardo O, Manenschijn JA, Fernandez-Pena C, Talavera A, Kichko T, Navia B, Sanchez A, Senaris R, Reeh P, Perez-Garcia MT, Lopez-Lopez JR, Voets T, Belmonte C, Talavera K, Viana F. TRPA1 channels mediate acute neurogenic inflammation and pain produced by bacterial endotoxins. *Nat Commun* 2014; 5:3125.
33. Barajon I, Serrao G, Arnaboldi F, Opizzi E, Ripamonti G, Balsari A, Rumio C. Toll-like receptors 3, 4, and 7 are expressed in the enteric nervous system and dorsal root ganglia. *J Histochem Cytochem* 2009; 57:1013–1023.
34. Muller PA, Koscsó B, Rajani GM, Stevanovic K, Berres ML, Hashimoto D, Mortha A, Leboeuf M, Li XM, Mucida D, Stanley ER, Dahan S, Margolis KG, Gershon MD, Merad M, Bogunovic M. Crosstalk between muscularis macrophages and enteric neurons regulates gastrointestinal motility. *Cell* 2014;158:300–313.
35. Gabanyi I, Muller PA, Feighery L, Oliveira TY, Costa-Pinto FA, Mucida D. Neuro-immune interactions drive tissue programming in intestinal macrophages. *Cell* 2016;164:378–391.
36. Caporaso JG, Kuczynski J, Stombaugh J, Bittinger K, Bushman FD, Costello EK, Fierer N, Pena AG, Goodrich JK, Gordon JI, Huttley GA, Kelley ST, Knights D, Koenig JE, Ley RE, Lozupone CA, McDonald D, Muegge BD, Pirrung M, Reeder J, Sevinsky JR, Turnbaugh PJ, Walters WA, Widmann J, Yatsunencko T, Zaneveld J, Knight R. QIIME allows analysis of high-throughput community sequencing data. *Nat Methods* 2010;7:335–336.
37. Kuczynski J, Stombaugh J, Walters WA, Gonzalez A, Caporaso JG, Knight R. Using QIIME to analyze 16S rRNA gene sequences from microbial communities. *Curr Protoc Bioinformatics* 2011, Chapter 10:Unit 10.7.
38. Aronesty E. Comparison of sequencing utility programs. *Open Bioinformatics J* 2013;7:1–8.
39. Martin M. Cutadapt removes adapter sequences from high-throughput sequencing reads. *EMBnet J* 2011; 17:10–12.
40. Edgar RC, Haas BJ, Clemente JC, Quince C, Knight R. UCHIME improves sensitivity and speed of chimera detection. *Bioinformatics* 2011;27:2194–2200.
41. Edgar RC. Search and clustering orders of magnitude faster than BLAST. *Bioinformatics* 2010;26:2460–2461.

---

Received November 17, 2017. Accepted September 10, 2018.

#### Correspondence

Address correspondence to: Takanori Kanai, MD, PhD, or Tomohisa Sujino, MD, PhD, Division of Gastroenterology and Hepatology, Department of Internal Medicine, Keio University School of Medicine, 35 Shinanomachi, Shinjuku, Tokyo 160-8582, Japan. e-mail: [takagast@keio.jp](mailto:takagast@keio.jp) or [tsujino1224@keio.jp](mailto:tsujino1224@keio.jp); fax: (81) 3-3353-6247.

#### Acknowledgments

The authors thank Atsushi Hayashi, Takahiro Suzuki, Yuko Homma, and Moeko Nakashima for technical assistance; Hisato Iriki for technical help with skin immune cell analyses; Nobuhiko Kamada (University of Michigan), Daniel Mucida, and Mariya London (The Rockefeller University) for reading the manuscript; and Akihiko Yoshimura (Keio University) for valuable comments. The authors thank the Edanz Group ([www.edanzediting.com/ac](http://www.edanzediting.com/ac)) for editing a draft of this manuscript.

Present address of Tadakazu Hisamatsu: The Third Department of Internal Medicine, Kyorin University School of Medicine, Tokyo, Japan.

#### Author contributions

Hiroki Kiyohara designed, performed, and analyzed most experiments and prepared the figures; Toshiaki Teratani and Mari Mochizuki Arai helped to analyze experiments; Ryo Aoki helped with fecal transfer experiments and Kentaro Miyamoto performed fecal 16S ribosomal RNA sequencing; Ena Nomura, Yosuke Harada, and Yuzo Koda performed bone marrow transplantation experiments; Yohei Mikami, Shinta Mizuno, Makoto Naganuma, and Tadakazu Hisamatsu were involved in scientific discussions; Tomohisa Sujino and Takanori Kanai conceived and supervised the project; and Tomohisa Sujino wrote the manuscript.

#### Conflicts of interest

The authors disclose no conflicts.

#### Funding

This work was supported by Grants-in-Aid 17K19668 and 17H05082 (T.S.), 17K15966 (S.M.), and 15H02534 (T.K.) from the Japanese Society for the Promotion of Science, the Japan Agency for Medical Research and Development grants 17929894 (T.S.) and Crest-16813798 (T.K.), the Applied Enzyme Foundation (H.K.), the Yakult Bioscience Research Foundation (T.K.), the Keio University Medical Science Fund (Sakaguchi Memorial), the Takeda Science Foundation, the Mochida Memorial Foundation, and the Astellas Foundation (T.S.).